RC22835 (W0307-015) July 1, 2003
Physics

IBM Research Report

"Dressed-atom" Lasers in Symbiotic Stars

P. P. Sorokin[1] , J. H. Glownia[2]

[1] IBM Research Division,
P. O. Box 218,
Yorktown Heights, NY
10598-0218

[2] Los Alamos National Laboratory,
P. O. Box 1663, Los Alamos,
NM 87545-1663

Research Division
Almaden - Austin - Beijing - Delhi - Haifa - India - T. J. Watson - Tokyo - Zurich

Astronomy & Astrophysics manuscript no. aah3389˙rev April 20, 2003

"Dressed-atom" lasers in symbiotic stars

P. P. Sorokin[1] and J. H. Glownia[2]

[1] IBM Research Division, P. O. Box 218, Yorktown Heights, NY 10598-0218, USA
e-mail: sorokin@us.ibm.com
[2] Los Alamos National Laboratory, P. O. Box 1663, Los Alamos, NM 87545-1663, USA
e-mail: jglownia@lanl.gov

Received 2002; accepted 2003

Abstract. It is shown that a model recently proposed for two-level-atom *lasers without inversion (LWI)* in Space (Sorokin & Glownia 2002) gains significant credibility when the model is instead constructed on the basis of atoms simultaneously saturated on two atomic transitions sharing a common level. The principal advantage attained by considering the atoms in the model to have three active levels rather than two is that the pumping efficiency no longer rapidly decreases with increasing power of the coherently generated light beam(s). The powerful "dressed-atom" approach for analyzing the physics of atoms strongly driven by resonant light beams (Cohen-Tannoudji & Reynaud 1977) provides a direct and insightful way to understand both this effect and the remarkable transparency that occurs at the bare-atom resonance frequencies ω_o and ω'_o in such systems. Both features make it possible for a coherently phased, dressed-atom gas to exhibit laser emission at ω_o and ω'_o, provided there exists a suitable independent pumping mechanism which can "donate" photons to the laser beams at a sufficiently high rate. It is shown that the nonlinear processes of *stimulated hyper-Raman scattering (SHRS)* and *stimulated broadband Raman scattering (SRS)* are generally effective means of converting incoherent pump light into coherent dressed-atom laser light, provided that the frequencies of the former and the latter are close together. This requirement would be optimally satisfied, for example, if the incoherent pump light were the strong fluorescence at ω_o and ω'_o produced via electron impact excitation (EIE) in an ionized plasma, since pump and laser frequencies would here differ at most by the Doppler width $\Delta\nu_D$. In the present paper, the emphasis is placed on exploring whether dressed-atom lasers could play important roles in exciting the strong far-ultraviolet (FUV) emission lines seen in symbiotic stars. A pure hydrogen symbiotic star model is first considered. It is shown that very high optical gain should exist for Lyα dressed-atom laser emission, with amplification mostly occurring within short distances of the H I/H II interface, as the laser beams propagate away from the latter. The pump mechanism for the Lyα laser emission would here be either SHRS or SRS. The pump light would be Lyα fluorescence generated within the ionized region. It is next explained that if Lyα dressed-atom laser emission is present, one could also expect Hα dressed-atom laser emission to occur. A laser-based interpretation is offered for the puzzling Hα line profile variations observed with changes in orbital phase in the eclipsing symbiotic star SY Mus. The strong C IV FUV doublet emission is considered next. It is concluded that C IV dressed-atom laser emission in symbiotic stars could theoretically also be present, with amplification here occurring along straight-line paths contained within that part of the ionized hydrogen plasma in which C IV is the dominant carbon species. The pumping mechanism in this case could only be SHRS, with the pump light being C IV fluorescence generated via EIE in the C IV-dominant region. Under the assumption that an analogous scenario would apply in the case of the O VI FUV doublet emission, an interpretation is given for the spectral structure observed on the 6825-Å Raman line in RR Tel. A new nonlinear process, *stimulated radiation pressure scattering (SRPS)*, is proposed to explain the observation that, in a few symbiotic stars, there occurs almost total absorption of the background continuum level in two comparatively narrow spectral regions, each blueshifted by the same amount from a component of an FUV doublet. A high quality C IV spectrum of EG And is analyzed on the basis of this new nonlinear process.

Key words. Atomic processes – radiation mechanisms: non thermal – stars: individual: SY Mus – stars: individual: RR Tel – stars: individual: EG And

1. Introduction

In a recently published paper (Sorokin & Glownia 2002 – hereafter referred to as S&G I), a new idea was suggested to explain relatively intense, narrow-band emission lines radiated by certain space objects. Specifically considered in S&G I were the strong O VI (1032 Å, 1038 Å) doublet emission that dominates the far-UV (FUV) spectra of some symbiotic stars (*e.g.* RR Tel), and the sharp, anomalously strong Hα emission line that is occasionally seen in reddened, early-type stars. It was proposed that these emissions represent spherically expanding output beams of so-called "lasers without inversion (LWI)" – the latter being located near certain very bright stars and being pumped by the blackbody continuum light emitted by

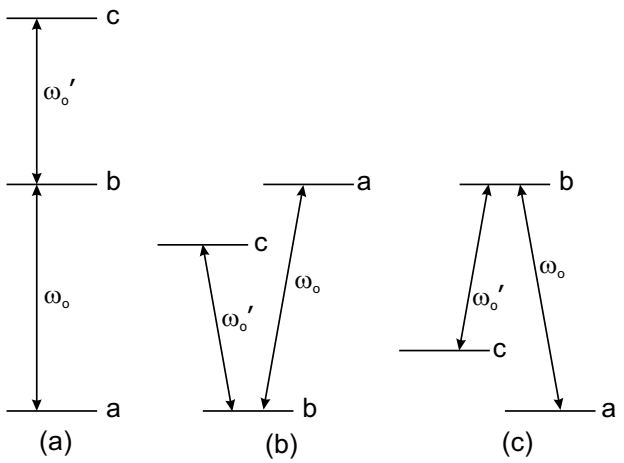

Fig. 1. Energy level structures for (a) cascade-, (b) V-, and (c) Λ-type three-level atoms.

those stars. A reasonably complete discussion was presented in S&G I of the essential physics that underlies the operation of an LWI. In general, any viable LWI scheme must include a photonic process that produces complete transparency at the lasing frequency, a condition usually referred to as "electromagnetically induced transparency" or EIT. In addition, there must exist a credible pumping mechanism and also a well defined source of pumping energy.

In Sect. 4 of S&G I, a lengthy description was given of some of the techniques that have been developed for inducing EIT in three-level systems. The relative energies and parity assignments of the atomic levels in a three-level system determine whether it is to be classified as a "cascade"-type, "V"-type, or "Λ"-type system (Fig. 1). In each of these types, the parities of two of the levels are taken to be the same, with the third being opposite. Two of the three transitions are thus dipole allowed; the third (the *ac* transition) is dipole forbidden. In principle, it should be quite straightforward to establish a condition of EIT in a tenuous gas of three-level atoms in Space. As noted at the end of Sect. 4 in S&G I, "... co-propagation of two resonantly-tuned, monochromatic laser beams through a tenuous gas of three-level atoms accomplishes one major step needed to realize an LWI in space – it removes in principle all attenuation (loss) for the two beams as they propagate away from stars that provide the pumping power required for amplification of the beams." This induced transparency occurs less as a result of saturation (*i.e.* equaling of the populations in the upper and lower levels of an unperturbed atomic transition), and more through quantum interference. The two laser beams effectively drive all atoms of the gas into a stable "coherently-phased population state". In this state, the wavefunctions of all the atoms in the gas become linear combinations of the unperturbed ("bare-atom") wavefunctions of the three levels. Atoms coherently phased by this method are commonly referred to as "dressed atoms", and sometimes also as "coherently trapped atoms". In the present paper, use of the former term is generally favored.

Although the discussion in Sect. 4 of S&G I was entirely focused on the establishment of EIT in three-level atomic systems, the need to find a credible pumping mechanism for an LWI in Space prompted the authors at that point to consider the possibility that an LWI might be realized with an even simpler system – a gas of two-level atoms. It was noted in S&G I that complete transparency in the vicinity of the resonance frequency ω_o of a two-level atom can be induced in a gas of such atoms simply by propagating through the gas a narrow-band laser beam tuned to ω_o. However, unlike what happens when EIT occurs in three-level atomic systems, EIT in two-level gases is invariably accompanied by heavy saturation of the transition, which in turn leads to a rapid drop off in the efficiency of the stimulated hyper-Raman scattering (SHRS) process proposed as the LWI pumping mechanism in S&G I. This problem with the two-level-atom LWI scheme was fully recognized in S&G I, and it was proposed that, as the power in the beam at ω_o increases, a related process, four-wave mixing (FWM), becomes the dominant nonlinear process that transfers power from the incoherent pump source to the coherently generated beam at ω_o. However, the calculation given in Appendix A of S&G I showed that the FWM process also strongly saturates, hinting that in future studies one might explore whether there exist other modifications of the LWI scheme proposed in S&G I that can account for lasing in a space object that emits narrow-band light at an intensity exceeding that of the illuminating star continuum level by several orders of magnitude, as occurs in each of the three symbiotic stars considered in S&G I, for example.

One of the main goals of the present paper is to show that there indeed exists a simple modification of the SHRS-based scenario proposed in S&G I that does allow incoherent pump light to be converted into narrow-band laser light at very high power levels. Specifically, it will here be outlined that saturation of a laser in space comprising a gas of coherently phased, three-level atoms (*i.e.* a "dressed-atom" laser) can be completely avoided. In this new scheme, the same basic SHRS pumping mechanism now operates in the spectral vicinity of *each* transition, converting incoherent pump light into coherent laser light at *both* allowed transition frequencies ω_o and ω_o'. It is shown that the dressed-atom structure allows this "dual" SHRS pumping process to continue to operate with high efficiency, even at the highest laser light intensity levels. Since the dressed-atom gas is fully transparent at ω_o and ω_o', the amplified beams can propagate through space without being attenuated.

In S&G I, the principal aim was to suggest that some superintense narrow-band emissions seen in space objects might represent coherently generated LWI light. In the present paper, having access to what we believe is a better theoretical model (*i.e.* dressed-atom lasers), we continue with equal enthusiasm to explore the same general exciting possibility. However, the focus is here placed entirely on symbiotic star systems, because of the unique physical characteristics these space objects possess that would increase the *a priori* likelihood that they could display laser emission. Section 2 is entirely devoted to an analysis of the possibility of laser emission in symbiotic stars. A pure hydrogen symbiotic star model is first considered.

It is shown that very high optical gain should exist for Lyα dressed-atom laser emission, with amplification mostly occurring within short distances of the H I/H II interface, and with the pump light for the SHRS pumping mechanism being Lyα fluorescence generated within the ionized region. It is next explained that if Lyα dressed-atom laser emission is present, one should also expect Hα dressed-atom laser emission to occur. Assuming the latter happens, an interesting interpretation can be given of the puzzling Hα line profile variations observed with changes in orbital phase in the eclipsing symbiotic star SY Mus. The strong C IV FUV doublet emission is considered next. It is concluded that C IV dressed-atom laser emission in symbiotic stars could theoretically also be present, with amplification here occurring in straight-line paths contained within that part of the ionized hydrogen plasma in which C IV is the dominant carbon species. The pump light for the SHRS pumping mechanism would be C IV fluorescence generated via EIE in the C IV-dominant region. Under the assumption that an analogous scenario would apply in the case of O VI FUV doublet emission, an interpretation is given for the spectral structure observed on the λ"6825" Raman line in RR Tel.

At the conclusion of Sect. 2, a new nonlinear process, *stimulated radiation pressure scattering (SRPS)*, is proposed to explain the observation that in symbiotic stars there (sometimes) occurs almost total absorption of the background continuum level in two comparatively narrow spectral regions, each blueshifted by the same amount from a component of an FUV doublet. A high quality C IV spectrum of EG And is analyzed on the basis of this new nonlinear photonic scheme, which, although relying upon different physical principles from those involved in dressed-atom laser emission, appears to be an *a priori* equally viable photonic process.

To try to identify a mechanism which would allow a space laser beam to be amplified without saturation occurring, we have found it most helpful to use the powerful "dressed-atom" approach for analysis of resonantly driven three-level systems, an approach that was proposed and explained in an illuminating paper published several years ago (Cohen-Tannoudji & Reynaud 1977 – hereafter referenced as C-T&R). This classical paper therefore forms the basis for Sect. 3 of the present paper. In that section, it is explained how one first constructs a foundation for the dressed-atom approach by considering an infinite lattice of "multiplicities" $\varepsilon_{n,n'}$ representing states of a system comprising an atom plus the two resonant laser fields with which it interacts. Each multiplicity consists of a threefold degenerate set of states. Each such state can be represented by a ket of the form $|l, n, n'\rangle$, corresponding to an atom in level l ($l = a, b, c$ - see Fig. 1) in the presence of n photons at ω_o and n' photons at ω'_o, with an unperturbed energy $E_l + n\omega_o + n'\omega'_o$ (taking $\hbar$=1). The threefold degenerate states comprising a given multiplicity depend upon whether the system being considered is of cascade-type, V-type, or Λ-type. For cascade-type systems (the only type explicitly considered in C-T&R), one has

$$\varepsilon_{n,n'} = \left\{ |a, n+1, n'\rangle, |b, n, n'\rangle, |c, n, n'-1\rangle \right\}. \qquad (1)$$

In the dressed-atom approach, one is really seeking to find the eigensolutions of the combined system of atom and monochromatic driving fields. The next step one takes is therefore to calculate how the multiplicities $\varepsilon_{n,n'}$ become perturbed by the presence of the two resonant laser beams at ω_o and ω'_o. A comparatively simple situation results when the so-called "secular approximation" is made, that is, when it is assumed that a quantity termed the "generalized Rabi frequency" Ω_1 is large compared to either of the radiative decay rates for the transitions *ab* and *bc*. (As already mentioned, it is here assumed that for all three types of atom structures the *ac* transition is radiatively forbidden.) In the presence of the resonant laser fields, each threefold degenerate multiplicity splits into three new states (the "dressed-atom" states) $|i, n, n'\rangle$ ($i = 1, 2, 3$), with the separation in energy between adjacent states in a given multiplicity being $(1/2)\Omega_1$. From the expansions of the dressed-atom states as linear combinations of the bare-atom states, one can determine the rates of all possible spontaneous emission decays from the three perturbed states of $\varepsilon_{n,n'}$ to lower multiplicities, *i.e.* one can determine the fluorescence spectra $F_{ab}(\omega)$ and $F_{bc}(\omega)$ of the dressed-atom system. For cascade-type atoms, C-T&R also show that (again, when the secular approximation holds) one can easily obtain expressions for the steady-state populations $\sigma^o_{ii}(n, n')$, which, to a very good approximation, can be factorized as:

$$\sigma^o_{ii}(n, n') = \{\pi_i\}\, p_o(n) p'_o(n'), \qquad (2)$$

where $p_o(n)$ and $p'_o(n')$ are the distributions of the photon numbers n and n', and π_i gives the steady-state probability that the i'th state in any perturbed multiplicity is occupied. Simple formulas for the π_i for cascade-type systems derived in C-T&R show that these quantities depend only on the bare-atom radiative decay rates and on the ratio of the Rabi frequencies of the two applied resonant laser beams.

In Sect. 4, the spectral properties of Λ- and V-type dressed-atom gases are considered. It is shown that for these systems, the quantities π_i can only have the values 0, 1, and 1/2 - making analyses of dressed-atom spectra generally much simpler than for cascade-type systems. From diagrams analogous to the one used in Sect. 3 to show the allowed spontaneous emission transitions from the perturbed $\varepsilon_{n,n'}$ states of cascade-type atoms, one can determine the fluorescence spectra of Λ- and V-type dressed atoms. In this connection, the Λ-type structure is especially interesting, because *no* fluorescence is emitted by dressed atoms of this type. Utilizing the appropriate dressed-atom spontaneous emission decay diagrams, and recognizing that the π_i values can only be 0, 1, or 1/2, one can immediately determine the linear absorption spectra for both Λ- and V-type dressed atoms in the vicinities of ω_o and ω'_o. For both, absorption occurs in four narrow bands centered at $\omega_o \pm (1/2)\Omega_1$ and $\omega'_o \pm (1/2)\Omega_1$. Although the absorption bands are shifted away from the bare-atom positions, they remain undiminished in strength. This is the underlying reason preventing saturation from occurring during SRS or SHRS pumping of a dressed-atom laser.

Having acquired basic knowledge about the absorption and fluorescence properties of dressed atoms, one is prepared to inquire how a gas of such atoms would respond to the additional presence of intense incoherent pump light at intensity levels believed to be present in symbiotic stars (Sect. 2). Both

linear and nonlinear optical pumping processes which potentially could provide gain at ω_o and ω_o' in a gas of V-type or Λ-type dressed atoms via absorption of such pump light are considered in Sect. 5. It is shown that while SHRS is the only optical pumping mechanism that could excite V-type dressed-atom laser emission in symbiotic stars, there is a potentially even stronger mechanism, stimulated broadband Raman scattering (SRS), that could provide effective pumping for Λ-type dressed-atom lasers in such systems. The Lyα laser discussed in Sect. 2 could therefore theoretically be as effectively pumped via SRS as by SHRS. In Sect. 5, brief mathematical "proofs" are also offered showing why the atoms of a coherently phased gas remain "dressed" as photons are "donated" to the laser beams via either SRS or SHRS.

In Sect. 6, we summarize the main ideas and conclusions of the present paper.

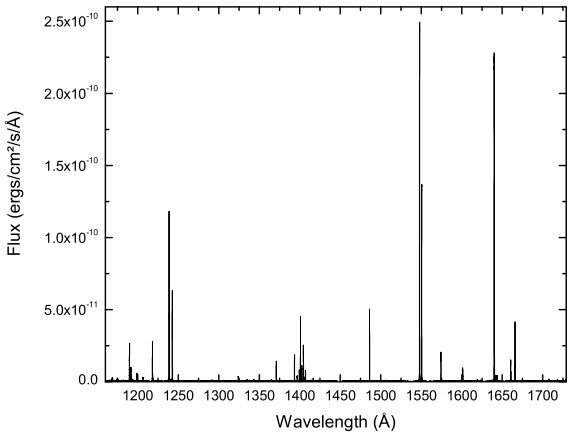

Fig. 2. *STIS* spectrum of RR Tel. Data set: **O5EH01010** downloaded from the *MAST Scrapbook* (http://archive.stsci.edu/scrapbook.html).

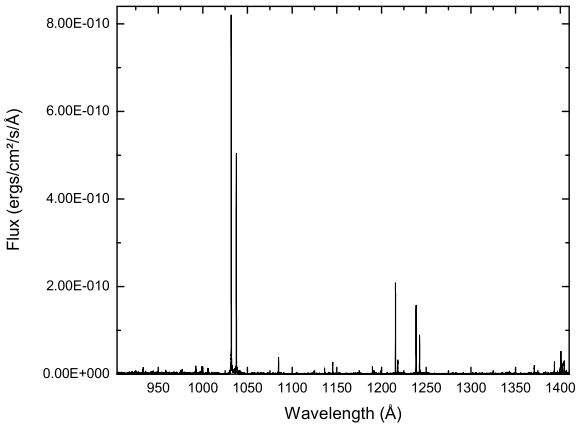

Fig. 3. *TUES* spectrum of RR Tel. Data set: **tues2218_1** downloaded from the *MAST Scrapbook* (http://archive.stsci.edu/scrapbook.html).

2. Far-UV (FUV) emission doublet intensities in symbiotic stars

2.1. Excitation mechanisms for the FUV emission doublets in symbiotic stars: ionization/recombination (I/R), electron impact excitation (EIE), and nonlinear photoexcitation (NLP) compared in a pure hydrogen model

In the FUV spectra of virtually all symbiotic stars, the C IV ($\lambda\lambda$1548, 1551) emission doublet is almost always strongly seen. The N V ($\lambda\lambda$1239, 1243) emission doublet is also frequently present, but its intensity is usually less than that of the C IV doublet (Fig. 2). The O VI ($\lambda\lambda$1032, 1038) emission doublet only appears in symbiotic stars having very hot white dwarf temperatures, such as RR Tel. However, not all such stars display this emission (*e.g.* RW Hya). When present, the O VI doublet is frequently the strongest emission feature in the FUV spectrum (Fig. 3). Throughout the entirety of Sect. 2, the main emphasis will be placed on exploring in a very general way whether there exists even a remote chance that nonlinear photonic mechanisms could play important roles in exciting strong emission lines observed in symbiotic stars, including the three above mentioned emission doublets, all of which are produced by ions having three-level, V-type structures, as illustrated by the O VI energy level diagram shown, for example, in Fig. 9 of S&G I. With the exception of the strong λ1640 He II emission, all other emission lines seen in Figs. 2 and 3 occur on partially forbidden transitions and therefore probably result from either EIE or electron-ion recombination, as has long been assumed in the symbiotic star literature.

We now focus on the simplest type of model for a symbiotic star nebula, *i.e.* one that contains only hydrogen atoms. Our analysis here will be based upon a symbiotic star model amenable to analytic solutions that was first suggested in Seaquist *et al.* (1984) and in Taylor & Seaquist (1984). These authors represent a symbiotic star by a cool red giant undergoing uniform, spherically symmetric, mass loss of hydrogen, with the H-atom gas density $n_H(x)$ in the outgoing wind being therefore given by

$$n_H(x) = \frac{\dot{M}}{4\pi m_H v x^2} \quad , \tag{3}$$

where x is the radial distance from the mass-losing star, $\dot{M}$ is the mass-loss rate, and v is the constant wind velocity. A hot white dwarf emitting L_{ph} hydrogen ionizing photons per second is located a distance a from the cool star and intercepts part of the wind from the latter. It is assumed that no separate wind emanates from the hot star itself. A parameter X is defined that determines the location of the ionization front in the model. This parameter is given by the expression

$$X = \frac{4\pi m_H^2}{\alpha_B} a L_{ph} \left(\frac{\dot{M}}{v}\right)^{-2} , \tag{4}$$

where α_B is the recombination coefficient to all but the ground state of hydrogen. The position of the ionization front is given

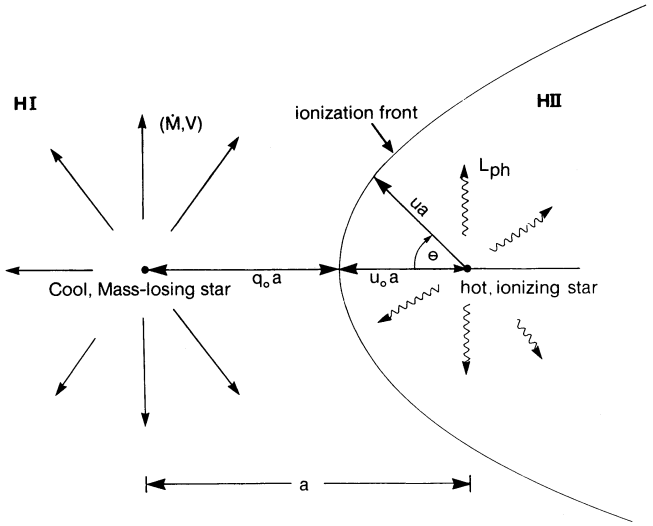

Fig. 4. Schematic of the pure hydrogen symbiotic star model. Reproduced from Fig. 1 of Taylor & Seaquist (1984).

by the expression

$$f(u,\theta) = X, \tag{5}$$

with the function *f(u,θ)* being that given in Eq.(5) of Taylor & Seaquist (1984). (The expression for *f(u,θ)* for the case $\theta \neq 0, \pi$ contains a misprint in both Seaquist *et al.* (1984) and Taylor & Seaquist (1984). A correction was published as an Erratum in 1987, ApJ, 317, 555.) The parameters u and θ are shown in Fig. 4. Characteristic shapes of the ionized nebula for three ranges of the parameter X are shown in Fig. 5.

Let us now examine the nebular structure described by the above model for a set of parameter values that could reasonably characterize an s-type symbiotic star. We assume $\dot{M} = 10^{-5} M_\odot$/yr, α_B = 2.0 x 10^{-13} cm^3/sec, v = 10 km/sec, T_h =100,000°K, a= 5 x 10^{13} cm, and R_h= 0.1$R_\odot$. The values chosen for T_h and R_h imply that L_{ph} = 6.55 x 10^{46} photons/sec. From this and the other parameters chosen above, one calculates from Eq.(4) a value for X of 0.0014. The nebular structure of our example is therefore closest to the one shown at the top in Fig. 5. From Eq.(5) one finds that the H I/H II ionization front occurs at a distance r = 7 x10^{12} cm from the hot star along the direction $\theta = 0$, whereas along the direction $\theta = \pi$, the distance to the ionization front is r = 9.75 x 10^{12} cm, *i.e.* $u_{\theta=0}$ = 0.14, $u_{\theta=\pi}$ = 0.195. From Eq.(3), one sees that $n_H(a)$ =1.2 x 10^{10} cm^{-3}. The *radiation bounded* nebula in our model can well be approximated by a simple Strömgren sphere, since substitution of the symbiotic star parameters assumed above into the standard equation for the Strömgren radius r_S

$$r_S^3 = \frac{3L_{ph}}{4\pi n_H^2 \alpha_B} \tag{6}$$

yields the value r_S= 8.16 x 10^{12} cm.

Although no given symbiotic star can probably be very well represented by the oversimplified nebular model here being considered, it is at least fairly straightforward to determine what should be the relative importance of I/R, EIE, and NLP

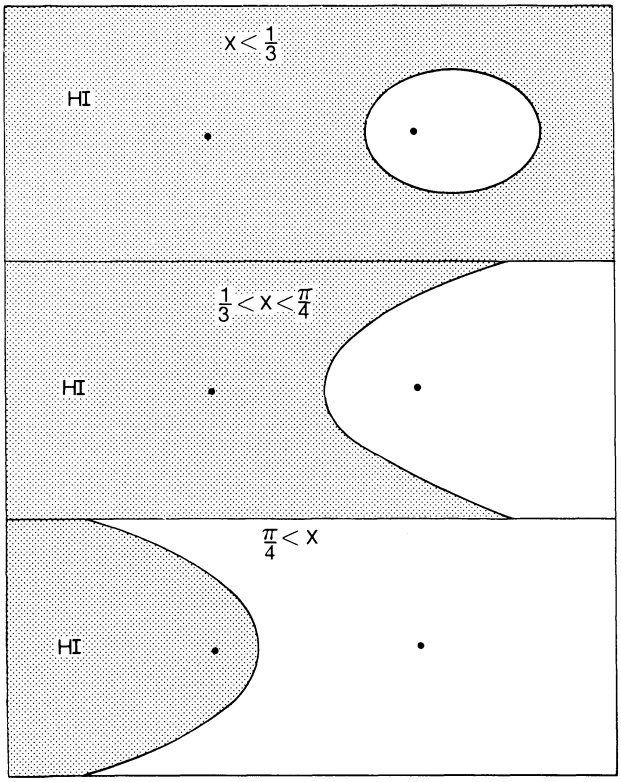

Fig. 5. Characteristic shapes of the ionized hydrogen nebula for three ranges of the parameter X. Reproduced from Fig. 2 of Taylor & Seaquist (1984).

in such a model. The most important photonic quantity to consider in this connection is the flux of Lyα photons crossing r_S. These photons are all generated inside the Strömgren sphere via either I/R or EIE. It is a standard approximation to assume that the rate at which Lyα photons generated by the first mechanism emerge from the entire Strömgren sphere surface is equal to L_{ph}. Thus the contribution to the Lyα flux crossing r_S from the I/R mechanism is $\varphi_{Ly\alpha}^{I/R}$ = 7.8 x 10^{19} photons cm^{-2} sec^{-1}, representing an optical power of 128 W/cm^2. In the standard Strömgren sphere scenario, the emerging Lyα photons would be distributed within a bandwidth $\Delta\nu_{Ly\alpha}^{I/R}$ corresponding to Doppler broadening of H atoms at the electron temperature T_e of the ionized plasma. For an assumed value $T_e \approx 10{,}000°K$, $\Delta\nu_{Ly\alpha}^{I/R}$ would be approximately 6 cm^{-1}.

Consider next the EIE contribution to the Lyα flux crossing r_S. The total rate ρ^{EIE} at which electrons located throughout the entire volume of the Strömgren sphere produce H-atom 2p excitations through collisions with neutral atoms existing in the plasma is approximately given by the following integration:

$$\rho^{EIE} = \int_0^{r_S} 4\pi r^2 n_e v_e^{th} \sigma_e^{2p} n_H^S(r) dr \quad . \tag{7}$$

Here $n_e \approx n_H$ is the density of electrons in the plasma, $v_e^{th} = (2kT_e/m_e)^{1/2}$ is the most probable thermal velocity of the electrons, $\sigma_e^{2p} \approx \pi a_o^2$ is the cross-section for electron impact excitation of H atoms to the 2p state, and $n_H^S(r)$ is the density of

hydrogen atoms within the ionized plasma of the Strömgren sphere. The functional dependence on r of $n_H^S(r)$ is given approximately by

$$n_H^S(r) \approx \frac{4\pi r^2 n_e^2 \alpha_B}{\alpha_0 L_{ph}} \quad , \tag{8}$$

where $\alpha_0 \approx 6.8\text{x}10^{-18}\text{cm}^2$ is the average H-atom photoionization cross-section. Evaluation of the integral in Eq.(7) with use of the above various parameter values yields the interesting result that $\rho^{EIE} = 4.29$ x 10^{45} photons/sec; *i.e.* only about 6.5 percent of the Lyα photons crossing the Strömgren sphere surface result from EIE. These would have the same spectral distribution as the Lyα photons resulting from the I/R mechanism. One should bear in mind that the relatively small fraction contributed by EIE to the total rate of Lyα photon production in the present model belies the general importance of this process as an emission-line-generating mechanism in symbiotic star nebulae. Relatively very few H atoms are present inside a Strömgren sphere, the *average* density in the present case being only $\approx$3.2 x10^4 cm^{-3}.

At first glance, it would seem relatively unimportant to know what exactly constitutes the main Lyα photon generation mechanism in the pure hydrogen symbiotic star model here being considered, inasmuch as all the Lyα light emerging from the Strömgren sphere should in principle immediately undergo elastic scattering and diffusion in the encompassing cloud of neutral hydrogen atoms that constitutes the cool star solar wind. However, let us now consider the possible roles that nonlinear photoexcitation (NLP) and dressed-atom laser emission could play in the model. A glance at the electronic energy level structure of the hydrogen atom (Fig. 6) shows that in principle this system is capable of supporting either Λ-type or V-type dressed-atom laser emission. However, although saturation of the nonlinear pumping process can equally well be avoided with both V- and Λ-type dressed-atom lasers, there is good reason for initially assuming the Lyα dressed-atom laser in our symbiotic star to be of Λ type. In Sect. 3 it is shown that while V-type dressed atoms strongly fluoresce, Λ-type dressed atoms do not. Thus Λ-type dressed-atom laser beams propagating in the solar winds of symbiotic stars should not be subject to extra attenuation due to a process that transfers power from the beams to support dressed-atom fluorescence, unlike what theoretically must happen in the case of V-type dressed-atom laser beams. However, the tentative conclusion just made that symbiotic star dressed-atom lasers must necessarily be based upon Λ-type systems will shortly come under further scrutiny, when we consider the possibility that Hα dressed-atom laser beams are also generated in these systems.

For the moment, let us continue to explore how generation of Lyα dressed-atom laser light might occur in the pure hydrogen symbiotic star model here being considered. For definiteness, let us assume the dressed-atom laser emission to occur on the transitions F=1$\Leftrightarrow$F'=1 and F=0$\Leftrightarrow$F'=1 of $1\ ^2S_{1/2} \Leftrightarrow 2\ ^2P_{3/2}$, these being stronger than the transitions connecting the $1\ ^2S_{1/2}$ hyperfine levels to F'=1 of $2\ ^2P_{1/2}$. To simplify the discussion at the outset, let it temporarily be assumed that generation of Lyα dressed-atom laser light commences at all points of the Strömgren sphere surface r_S, with propagation and amplification then occurring in directions that point radially away from the hot star. Amplification should everywhere continue to occur for a characteristic radial length that will be analyzed below. However, at larger radial distances, the dressed-atom laser intensity should start to weaken, due both to the effects of pump power depletion and to the unavoidable $1/r^2$ intensity fall off that accompanies a spherically expanding wave front. Eventually, when the dressed-atom laser intensity falls below a critical level needed for the so-called *secular approximation* to apply (see Sect. 3), the condition of EIT can no longer be maintained, and the laser light then starts to become elastically scattered in the same manner as would occur for incoherent Lyα light.

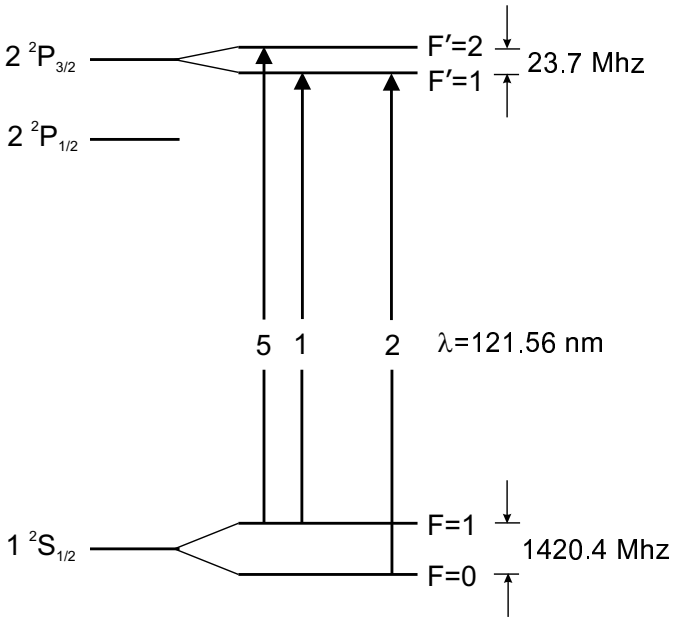

Fig. 6. Energy levels involved in 1s-2p transitions of hydrogen (not drawn to scale). The numbers in the arrows indicate the relative transition intensities. Adapted from Fig. 2 of Eikema *et al.* (2001).

In this scenario, the flux of incoherent Lyα photons emerging from the Strömgren sphere surface constitutes the pumping light. As this light diffuses outwards from r_S, it ideally should eventually become entirely converted to Lyα dressed-atom laser radiation via the nonlinear process of stimulated hyper-Raman scattering (SHRS). In Fig. 7 is shown both a schematic diagram of the unit SHRS process and a sketch depicting what a possible relationship of pump bandwidth to dressed-atom-laser bandwidth might be. The pump bandwidth is here assumed to be the $\approx$ 6 cm^{-1} spectral width spanned by the Lyα photons generated within the Strömgren sphere. However, let it also initially be postulated that *outside* of r_S the H-atom gas is at a temperature cold enough such that the effective Lyα fluorescence bandwidth is $\Delta\nu_n \approx 0.003$ cm^{-1}, the value that corresponds to natural lifetime broadening for this transition. We are temporarily making this patently unrealistic assumption that Doppler broadening of H atoms outside r_S can be completely neglected in order to obtain quickly a rough idea of what the dressed-atom-laser *optical gain* would be in

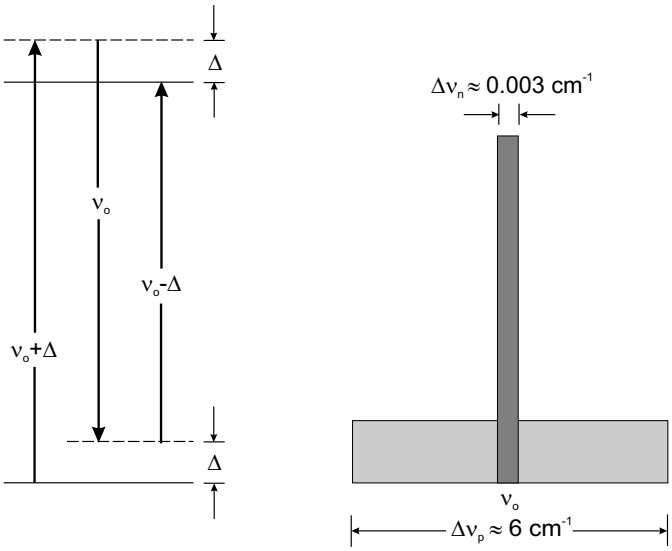

Fig. 7. (Left) - Diagram showing the energy-conserving, simultaneous, three-photon scattering process involved in SHRS pumping of dressed-atom lasers. Here ν_o represents either of the bare-atom frequencies, with Δ being the frequency offset from ν_o of either of two pump photons that are simultaneously absorbed while a photon is "donated" to the laser beam at ν_o. In the process, the atom becomes excited. (Right) – Schematic diagram showing relationship (not to scale) of generated narrow-band Lyα laser light to the pump radiation that drives it (see text).

the model under the most favorable circumstances. Later this particular assumption will be relaxed.

One can determine approximately what the optical gain of a Lyα dressed-atom laser based upon SHRS pumping should be in the symbiotic star model here being considered as follows. A formula for the gain coefficient due to SHRS is given, for example, in Eq. (5.22) of Hanna *et al.* (1979). Applied to the present case, this formula would appear as:

$$G_{HR} = g_{HR} I_p^2 = \frac{n_H \omega_o I_p^2 \mu^6 / 4\varepsilon_o^3 c^3 \hbar^5 \Gamma}{\Delta^4}. \qquad (9)$$

Throughout Hanna *et al.* (1979) SI units are employed. For convenience, we here do the same in estimating the SHRS optical gain for our hydrogen symbiotic star model. Thus $n_H \approx 1.64$ x 10^{16} m^{-3} is the hydrogen atom density at the $\theta = 0$ ionization front, $\omega_o = 1.55$ x 10^{16} radians/sec is the angular Lyα frequency, $I_p \approx 1.36$ x 10^6 W/m^2 is the total power per unit area of the Lyα radiation emerging from r_S, $\mu \approx 8$ x 10^{-30} Cm is the induced Lyα transition dipole moment (as obtained from Eq. (10) below), $\varepsilon_o = 8.85$ x 10^{-12} Fm^{-1} is the permittivity of free space, $c = 3$ x 10^8 m/sec is the velocity of light in vacuo, $\hbar = 1.05$ x 10^{-34} Jsec is the Dirac constant, $\Gamma \approx 0.6$ x 10^9 rad/sec is the Lyα natural linewidth expressed as an angular frequency, and $\Delta \approx 2.8$ x 10^{11} rad/sec is an average frequency offset (see Fig.7) which can be used together with the above value for I_p in Eq.(9) to approximate what in principle should be an integration of symmetrically offset pump pair frequencies over the entire $\approx$ 6-cm^{-1}-wide pump bandwidth. (Actual integration of the expression given in Eq. (9) leads to an infinite value because linewidths have not been included in the quantity Δ appearing as a fourth power in the denominator.) The value for μ assumed above follows from the standard equation

$$\mu^2 = \frac{1}{\tau_{rad}} \frac{3\pi\varepsilon_o \hbar c^3 g_u}{\omega_o^3 g_l}, \qquad (10)$$

where $\tau_{rad} \approx 10^{-9}$ sec is an approximate average radiative lifetime for the two Lyα doublet components, and g_u, g_l are upper and lower level degeneracies, which for simplicity are here taken to be the same.

Substitution of all the above values in Eq. (9) yields $G_{HR} \approx 3.5$ x 10^{-8} m^{-1}. The hyper-Raman gain given by Eq. (9) represents an *exponential* intensity gain per unit length, that is, in the absence of pump power depletion and/or saturation in the efficiency of the basic SHRS process, the intensity of a dressed-atom laser beam pumped by this process would increase by a factor $e^{G_{HR} l}$ in traveling a distance l. In nonlinear optics, it is conventional to assume that threshold for a nonlinear stimulated emission process like SHRS to occur with only a noise input signal is automatically reached when the beam has propagated a distance $l_{thr} \sim 30/G_{HR}$. This suggests that in the present case full intensity of a spherically expanding dressed-atom laser beam will occur shortly after the beam has radially propagated outwards from r_S a distance $l_{thr} \sim 0.86$ x 10^9 m, which is seen to be only about one percent of r_S itself. Thus for the idealized symbiotic star structure here assumed, dressed-atom laser emission should begin to occur just outside r_S, with full conversion of incoherent Lyα pump light into coherent dressed-atom laser light occurring within an additional propagation distance equal to a percent or so of r_S. At any distance from the hot star, the total power per unit area of the spherically expanding dressed-atom laser light would be roughly the same as what the incoherent Lyα pump light intensity would be in the complete absence of SHRS – about 136 W/cm^2 near r_S.

In Sect. 3 it is explained that a condition of EIT is maintained in a dressed-atom laser as long as the *secular approximation* ($\Omega_1 \gg \gamma, \gamma'$) holds. For a hydrogen dressed-atom laser, $\Omega_1 \sim 10\gamma, \gamma'$ should occur at a laser intensity ~100 mW/ cm^2. The dressed-atom laser radiation in the present model should thus in principle propagate without loss radially outwards until a total distance $r \sim 37 r_S \approx 6a \approx 3$ x 10^{14} cm from the white dwarf is reached. At larger values of r, the outwardly propagating spherical wave of Lyα dressed-atom laser light would in theory become increasingly subject to elastic scattering and diffusion due to hydrogen atoms present in the outer reaches of the red giant solar wind.

However, changes in the above picture become required when one takes into account both (a) the flow pattern of the red giant solar wind assumed in the model and (b) the fact that, in order for the model to be realistic, the Doppler broadening $\Delta\nu_D$ of the hydrogen atoms located outside r_S should be assumed to be much greater than $\Delta\nu_n$. With regard to the former, simple calculation shows that, in the absence of Doppler broadening, a Lyα dressed-atom laser beam that propagates along the direction $\theta = \pi/2$, for example, would be subject to a 0.0045-cm^{-1} resonance frequency shift in traversing the critical distance $l_{thr} = 0.86$ x 10^{11} cm. This shift is one-and-a-half times greater than the value $\Delta\nu_n = 0.003$ cm^{-1}earlier used to calculate

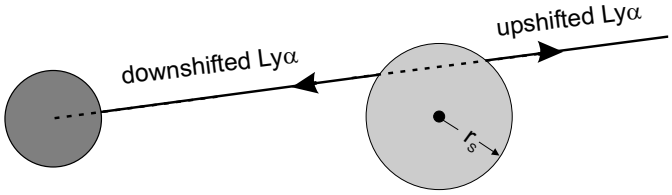

Fig. 8. Schematic diagram showing SHRS-pumped Lyα dressed-atom radiation propagating along a red giant solar wind ray that intersects the Strömgren sphere in two places. Laser beams propagate away from the latter in the two directions shown. Relative sizes shown of the red giant radius, Strömgren sphere radius, and binary star separation approximately correspond to those of the model assumed in the text.

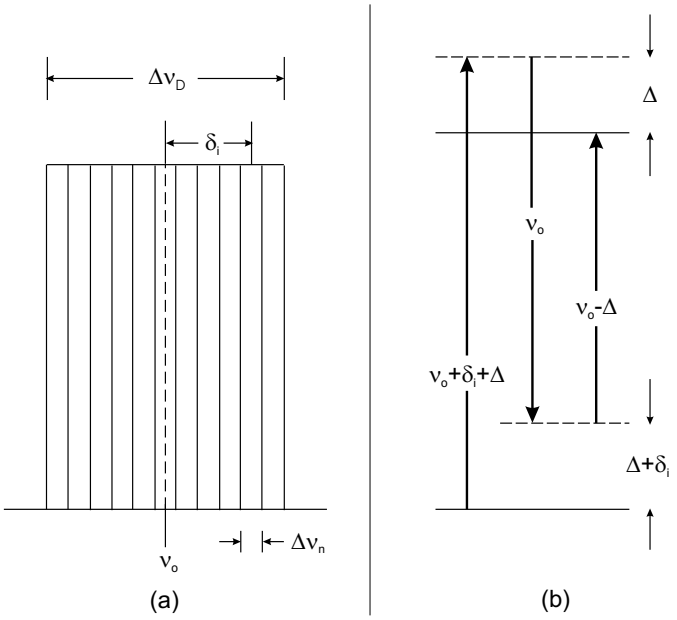

Fig. 9. (a) - Schematic diagram showing relationship of the Lyα natural linewidth $\Delta\nu_n$ to the Lyα Doppler width $\Delta\nu_D$ in the red giant solar wind outside the Strömgren sphere. (b) – Asymmetric SHRS scattering process by which atoms with frequencies offset by δ_i from ν_o can still contribute to the gain at ν_o.

Γ in Eq. (9). Thus, for a $\theta = \pi/2$ laser beam, the gain would additionally be lowered due to an inherently non-cancellable *inhomogeneous broadening* contribution to the linewidth. This effect would be zero if each Lyα dressed-atom laser beam were to propagate away from its point of origin on r_S along the line determined by the solar wind ray that intersects r_S at the same point (Fig. 8). Most of the gain would occur just outside each of the two points where each such solar wind ray intersects r_S. We thus here assume that the Lyα laser beams originating on the surface of r_S closest to the red giant propagate towards the latter in a convergent manner, while those emanating from the more remote surface of r_S propagate away from the symbiotic star system in a divergent manner. The former beams would be redshifted by 2.74 cm^{-1} from the system RV; the latter beams would be blueshifted from the RV by the same amount. It is likely that the highest Lyα intensity in the whole symbiotic star system would occur where the cone of converging dressed-atom laser beams originating from the surface of r_S nearest the red giant intersects the surface of the latter.

The contribution of Doppler broadening $\Delta\nu_D$ to the Lyα transition linewidth of the solar wind atoms would appear to have far more serious consequences in reducing the Lyα dressed-atom laser gain than the effect considered above. For example, if the Doppler broadening were 3 cm^{-1}, the critical length l_{thr} would be 8.6 x 10^{13} cm, which is greater than the separation between the two stars assumed in the model. To attempt to circumvent this difficulty, we here propose the following idea. Consider a dressed-atom laser beam propagating along a line determined by a solar wind ray, as outlined in the preceding paragraph. Conceptually divide the entire width $\Delta\nu_D$ into contiguous natural linewidth segments $\Delta\nu_n$ (Fig. 9a). Associated with the i'th segment is a hydrogen atom density n_H^i, with $\sum_i n_H^i = n_H$. The centermost segment will again contribute to the dressed-atom laser gain at the resonance frequency ν_o in the same manner as calculated before (*i.e.* with use of Eq. (9) and the parameter values earlier substituted), except that the value of n_H must now be taken to be roughly 1000 times smaller. However, *each* segment that is offset from ν_o by δ_i can also contribute roughly an equal amount to the gain at ν_o through the somewhat asymmetrical SHRS process shown in Fig. 9b. In this figure, an integration involving Δ over the whole Doppler width is implied. On the basis of this reasoning, it follows that the Lyα dressed-atom-laser gain will not be enormously reduced via any existing Doppler broadening of the H atoms in the solar wind. If the gain is sufficiently high for laser emission to occur on a narrow line spectrally contained within the centermost segment, the same argument implies that it will also be high enough for laser emission to occur on a narrow line contained within an adjacent segment. Thus, one expects the Lyα dressed-atom laser beam to have a spectral width that is orders of magnitude greater than $\Delta\nu_n$, and very likely as large as a considerable fraction of $\Delta\nu_D$. It should be noted that the general argument presented here is valid only because the SHRS process that produces the gain is nonlinear. Normal lasers require population inversions and are pumped by linear processes. For these, the optical gain is always inversely proportional to $\Delta\nu_D$.

An important point concerning possible Lyα dressed-atom laser operation in symbiotic stars is the following. In the field of quantum electronics (*e.g.* Fulton *et al.* 1995), it is known that EIT can be observed in Doppler-reduced experiments as long as the Rabi or Townes-Autler splitting is greater than the *residual two-photon linewidth* $\Delta\nu_{resD}$. The latter quantity is given by the expression

$$\Delta\nu_{resD} = |(k_1 \pm k_2)|\,\eta, \qquad (11)$$

where k_i is the wave number (ν_i/c) of the applied optical field E_i, which in the case of the symbiotic star model would be positive for a wave propagating away from r_S, and negative for a wave propagating towards it. The negative sign in Eq. (11) applies for V- and Λ-type systems, with the positive sign applying for cascade-type systems. In Doppler reduced experiments, η is the most probable thermal velocity $(2kT/m_a)^{1/2}$, with m_a the atomic mass. The frequencies of the transitions F=0$\Leftrightarrow$F'=1 and F=1$\Leftrightarrow$F'=1 in Fig. 6 are seen to be practically the same. Thus, for a Λ-type Lyα dressed-atom laser operating on these two transitions, and with the two laser beams co-propagating along

a solar wind ray, the residual two-photon linewidth $\Delta\nu_{resD}$ should be extremely small. One therefore deduces that a condition of EIT would be easily maintained as the Lyα laser beams propagate away from r_S along paths coincident with solar wind rays.

To the authors' knowledge, no conclusive report exists of narrow-band Lyα radiation ever having been detected in symbiotic stars. (The narrow-band Lyα emissions appearing in the spectra shown in Sect. 2 are usually identified as *geocoronal* Lyα emissions.) In view of the extensive amount of Lyα-photon elastic scattering that should be occurring in the far reaches of the red giant solar wind cloud, and the likelihood that the presence of some dust here might cause these photons to become absorbed before they are able to diffuse out of the cloud, the apparent absence of Lyα emission in symbiotic stars is perhaps quite understandable. One thus should here inquire what possible *observable* spectral features might conceivably be produced by the presence of Lyα dressed-atom laser radiation in symbiotic stars. For the simple hydrogen model here being considered, a possible effect to consider would be generation of Hα dressed-atom laser radiation in a three-level, *cascade-type* scheme (Fig. 1). As explained, for example, in Sect. 4 of S&G I, the presence of Lyα dressed-atom radiation generated in the manner discussed above would automatically establish a condition of EIT on the Hα transition. However, from Sect. 3 of the present paper, one also sees that actual pumping of the dressed-atom Hα laser must occur via SHRS conversion of broadband incoherent light present in the spectral vicinity of this transition. There are two spatially separated regions of the symbiotic star where Hα pumping possibly could occur. (1) The Hα transition could be pumped near r_S via incoherent Hα light emerging from the Strömgren sphere. An intense amount of such light is produced within the Strömgren sphere plasma by the same basic I/R and EIE mechanisms that generate copious amounts of Lyα light. The bandwidth of this Hα radiation should ideally again be the Doppler width of H atoms at a temperature corresponding to T_e of the plasma. In the present case, the incoherent Hα bandwidth would be about 1.1 cm^{-1}. (2) At first glance, it also seems reasonable that the Hα transition could be pumped by visible continuum light emitted by the red giant just outside the region of the latter's surface that is irradiated by the converging Lyα dressed-atom laser beams. It is therefore instructive to compare the intensities of these two possible Hα pump sources.

With regard to the first source, we assume the flux of incoherent Hα photons crossing r_S to be the same as the Lyα flux generated via I/R, that is, $\varphi_{H\alpha}^{I/R}$= 7.8 x 10^{19} photons cm^{-2} sec^{-1}. This is a power of 24 W/cm^2 distributed over a 1.1 cm^{-1} bandwidth. To make an estimate of the second source, one needs to assume a value for the temperature of the red giant. Choosing T_r = 3000°K, one finds the red star continuum flux emitted at its surface in the spectral vicinity of Hα to be roughly 3 x 10^{16} photons cm^{-2} sec^{-1} per cm^{-1}, which is seen to be negligible compared to the intensity of the first source.

Hydrogen Balmer-α emission *is* strongly seen in symbiotic stars, and its apparent intensity varies greatly with orbital phase in those systems which are known to be eclipsing. For example, in Fig. 10 (reproduced from Fig. 5 of Schmutz *et al.* (1994)) the Hα emission profile of the eclipsing s-type symbiotic star SY Muscae is shown as a function of orbital phase. The Hα intensity is strongest at *superior conjunction* (RV-phase 0.25), *i.e.*when the white dwarf is in front of the red giant, with both stars being in the line-of-sight. At this phase the spectrum is dominated by two relatively narrow components, whose peaks are separated by approximately 5 cm^{-1}. At a velocity roughly –100 km/sec relative to the systemic rest frame, an additional peak of much smaller intensity is seen to be present. With further advances in phase, the Hα-emission equivalent width steadily decreases, until a value near zero is reached at *inferior conjunction* (RV-phase 0.75), *i.e.* when the white dwarf is fully eclipsed by the red giant. (No measurements at RV-phase 0.75 are actually shown in Fig. 10. However, in Fig. 6 of Munari (1993) the Hα equivalent width in another eclipsing symbiotic star, EG And, is plotted for closely spaced phase changes throughout the complete orbiting cycle. The equivalent width again displays a maximum at superior conjunction, and a near zero minimum at inferior conjunction. The evolution of the Hα spectral profile along the orbiting cycle of EG And, shown in Fig. 4 of Munari (1993), is generally similar to the one for SY Mus shown in Fig. 10.)

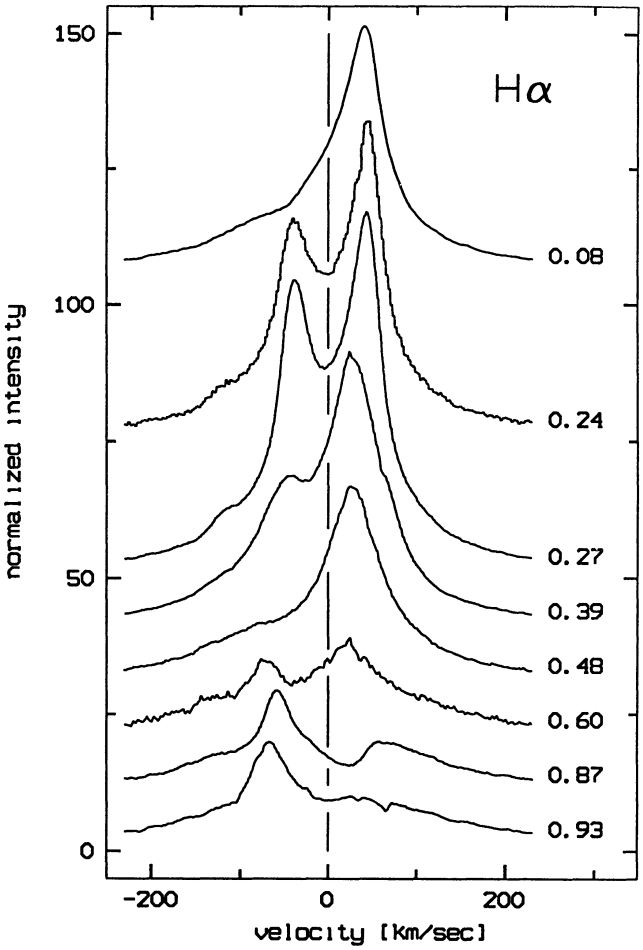

Fig. 10. Hα line profiles at various RV phases in SY Mus. Reproduced from Fig. 5 of Schmutz *et al.* (1994).

Schmutz *et al.* (1994) make no attempt to provide a convincing explanation for the puzzling line profile variations of Hα shown in Fig. 10. At this stage, we are only able to offer a totally speculative and non-rigorous interpretation of this same data, the basis of this interpretation again being the hypothesis that a significant part of the observed Hα emission might represent dressed-atom laser light. With regard to the *specific* hydrogen symbiotic star model we have here been studying, let us first of all consider what one would expect to see if *no* dressed-atom laser light were present. All the observed Hα light would then have to be generated via either I/R or EIE occurring within the Strömgren sphere plasma. In this case, one should observe basically the same Hα intensity during all phases of the orbiting cycle where the view of the entire Strömgren sphere remains unobstructed by the red giant. Assuming that the flow pattern of the 10 km/sec solar wind emanating radially outwards from the red giant remains the same within the Strömgren sphere, the peak of the Hα emission at superior conjunction would appear blueshifted by 10 km/sec from its position at *quadrature* (RV-phases 0 and 0.5). (A symbiotic star is viewed at quadrature when the line-of-sight to the system makes an angle of 90° with its axis.) There would seem to be no simple explanation for an apparent 5 cm^{-1} splitting at superior conjunction or at any other phase. It would also be difficult to account for the considerable spectral width variations that occur with changes in orbital phase, *e.g.* the fact that the width of the redshifted peak roughly doubles in going from superior conjunction to quadrature.

In attempting to interpret the data in Fig. 10 by postulating the existence of Hα dressed-atom laser emission in the pure hydrogen symbiotic star model, it is most natural to assume that the splitting of the main peaks seen at superior conjunction represents the frequency difference between an Hα laser beam propagating away from the red giant along a solar wind ray, and one that propagates towards the cool star. For the assumed 10 km/sec solar wind velocity in the model, the splitting between the peaks should be about 1 cm^{-1}. This would imply that the solar wind velocity in SY Mus must actually be about 50 km/sec. One can easily understand why the blueshifted peak is strongly present at superior conjuction. This is because an Hα laser beam originating at r_S and propagating away from both r_S and the red giant would have to be Doppler blueshifted from the system RV by 0.5 cm^{-1}. We will shortly below propose an explanation for the much smaller blueshifted peak seen at superior conjunction in Fig. 10 at ≈ -100 km/sec.

The real difficulty here is to account for the even stronger redshifted peak that is seen at superior conjunction. One can of course logically assume that there would be Hα laser beams originating at the surface of the Strömgren sphere facing the red giant and propagating towards the latter along the same directions it was earlier conjectured that the Lyα laser beams would follow. These would be Doppler downshifted from the system RV by 0.5 cm^{-1}, but would be undetectable at superior conjuction or at any other phase, since they would be intercepted by the red giant surface, if indeed they were able to propagate that far (*vide infra)*. It appears that the only possible way out of this impasse is to assume that Hα dressed-atom laser beams that propagate *away* from the red giant can also be generated near the same Strömgren sphere surface that *faces* the red giant. One would thus have counter-propagating Lyα and Hα dressed-atom laser beams in the vicinity of this surface. Paradoxically enough, although such Hα laser beams would be moving in the direction of the solar wind, they would still be Doppler *downshifted* by 0.5 cm^{-1} from the system RV, due to the presence of the intense counter-propagating Lyα laser radiation that plays the dominant role in "dressing" the hydrogen atoms. These redshifted Hα laser beams would then pass without attenuation through the Strömgren sphere and would thus in principle be directly detectable at superior conjunction.

To understand other features of the spectra shown in Fig. 10, one must consider some additional properties a cascade-type, dressed-atom laser would have. Reference was earlier made to that part of Sect. 3 in which the absorption spectrum of a resonantly driven, three-level, cascade-type atom is discussed. In that section, it is explained that if the Rabi frequencies of the two applied monochromatic beams are such that $\omega_1' \ll \omega_1$, then *all* linear absorption by the dressed atom occurs via an intense doublet whose components are symmetrically offset from ω_o' by (one-half) the generalized Rabi frequency Ω_1. That is, in the spectral vicinity of ω_o the atom would be totally non-absorbing. This was the basis of the statement made earlier that gain for an Hα cascade-type dressed-atom laser can result only from the presence of pump light existing in the spectral vicinity of this transition. In CT&R, the fluorescence spectrum of resonantly driven cascade-type atoms is also considered. For the same case $\omega_1' \ll \omega_1$ it is shown that the *intensity* of each fluorescent component about ω_o' is reduced by the factor $(\omega_1'/\omega_1)^2$. Thus, although Hα fluorescent emission apparently has to accompany the propagation of Hα dressed-atom laser beams in our symbiotic star model, the amount of such fluorescence generated would be greatly reduced if the Lyα laser beam intensity were at every point in the symbiotic star very much greater than that of the co-propagating (or counter-propagating) Hα laser beam at the same point. We assume this to be the case in the model.

Let us now consider what in principle should happen anywhere just outside the Strömgren sphere surface r_S where Hα dressed-atom laser light starts to become generated via SHRS. While its intensity is still very low, an Hα laser beam can propagate without being significantly attenuated along a solar wind ray a certain distance away from r_S. However, as the laser intensity increases to somewhat higher levels, Hα dressed-atom fluorescence will begin to occur, removing photons from the laser beam. This fluorescence would be isotropically emitted in all directions. In the rest frame of a dressed atom emitting such a fluorescent photon, the wavelength of the latter would be that of the laser beam driving the transition. However, as the fluorescent photon leaves the atom where it is generated, its wavelength will be Doppler shifted from that of the driving laser as a result of the relative motion of the atom with respect to the symbiotic star rest frame. Thus, for example, the dressed-atom fluorescence which would be produced by the 0.5-cm^{-1}-blueshifted Hα dressed-atom laser beams that propagate away from the system in the model would theoretically be viewable at superior conjunction as a separate small band that is *additionally* blueshifted by 0.5 cm^{-1} from the already blueshifted

Hα dressed-atom laser beams. This is our current interpretation of the small emission band seen at $\approx$ -100 km/sec at superior conjunction phase in SY Mus.

There is an inherent left-right asymmetry in the nonlinear model here being proposed which can possibly account for the following prominent feature of Fig. 10. In this figure, it is seen that at quadrature the redshifted emission is considerably stronger than the blueshifted emission. According to the model, *all* emission seen at quadrature must represent dressed-atom fluorescence. This is because the propagation directions of all Hα laser beams which potentially can be viewed directly would be confined within a cone which just subtends the Strömgren sphere and whose vertex is at the center of the red giant. Thus, for example, it is consistent with the model that in the top spectrum of Fig. 10 the red emission peaks at roughly the same wavelength that it does in the second and third spectra from the top. In each of the latter two spectra, the redshifted Hα emission largely represents laser emission. In the top spectrum it represents Hα dressed-atom fluorescence, which, as will be explained shortly, should mostly originate in a region that is relatively close to the area on the red giant surface that is irradiated by the converging rays of Lyα dressed-atom laser radiation. At quadrature, this fluorescence would be observed to have a peak coincident with that of all Hα laser radiation propagating in this region. It would not be subject to additional Doppler redshifting or blueshifting by the motion of the solar wind, since the latter occurs primarily at right angles to the line-of-sight.

The reason why more redshifted than blueshifted light is seen at quadrature has to do with the left-right asymmetry in the model. As the diverging blueshifted Hα laser beams propagate away from r_S, they become less intense, and so there is less dressed-atom fluorescence that is produced. However, the intensities of redshifted Hα laser beams propagating away from r_S towards the red giant are increased by the fact that these beams, following the Lyα laser paths, would tend to converge upon the red giant surface. However, as explained above, this would greatly increase the production rate of dressed-atom fluorescence. Some of the fluorescent photons created would be reabsorbed almost "on the spot" via SHRS-induced intensification of Hα laser beams propagating in one or both directions in the same spatial region where the photons are produced. This laser beam intensification would in turn lead to more dressed-atom fluorescence being produced, and so on. The above scenario somewhat hints that the density of Hα fluorescent photons emitted by dressed atoms might become significantly enhanced in a region that is not too far from the red giant via a form of photon trapping that superficially resembles that which is involved in the classical study of redistribution, in angle and frequency, of photons scattered between bound atomic states. In the case of dressed-atom fluorescence, the photons created are always produced with a Doppler frequency distribution that is centered at the wavelength of the dressed-atom laser driving the system. This would thus best correspond to the approximation of *complete redistribution* that is often made in classical studies of scattering by two-level atoms. However, there is one apparent difference that would exist between the photon-density-enhancing mechanisms in each case. In elastic scattering by two-level atoms, the photon density in a given region can be enhanced only via diffusional flow of photons from a region of higher photon density. By contrast, in the process by which the density of dressed-atom fluorescent photons could potentially become enhanced, the photons are initially transported to the region where the enhancement occurs via the dressed-atom laser beam. We have not performed any real calculations that would indicate the expected magnitude of such Hα dressed-atom fluorescence trapping in the pure hydrogen symbiotic star model. Nonetheless, we here end our discussion of this model by qualitatively outlining a likely steady-state scenario for this effect.

Just outside the surface of r_S that faces the red giant, redshifted Hα laser beams both co-propagate and counter-propagate along the directions of redshifted Lyα laser beams. (It is assumed that there are no blueshifted Lyα laser beams present in this region of the symbiotic star.) The co-propagating Hα laser beams eventually terminate in a relatively high density cloud of Hα fluorescent photons localized both within the truncated cone of Lyα laser radiation and relatively close to the red giant surface. The co-propagating Hα laser beams never reach the latter. A large fraction of the Hα fluorescent photons escape from the cloud and are seen, for example, as the redshifted emission at quadrature. The linewidth of this emission represents the Doppler width $\Delta\nu_D$ of H atoms in the solar wind. Those Hα fluorescent photons in the cloud that do not escape are absorbed via SHRS pumping of counter-propagating Hα laser beams. The latter escape the system by passing through the Strömgren sphere and are seen at superior conjunction.

In trying to make an *a priori* determination of the salient photonic properties of a pure hydrogen symbiotic star, we have not attempted to vary any parameters. Had the red giant solar wind velocity, for example, been chosen to be five times greater (which would have allowed a more realistic comparison with Fig. 10), the size of the Strömgren sphere would have become much larger, and the left-right asymmetry in the model would have correspondingly increased. The latter in turn would have produced a larger ratio of redshifted to blueshifted intensities in the model. It should also be noted that the postulated existence of Hα cascade-type dressed-atom laser beams in our symbiotic star model actually involves a *four-level* atomic scheme (one Hα frequency, two Lyα frequencies), and therefore, strictly speaking, may not allow analysis to be made on the basis of the ideal three-level-atom cascade scheme discussed in Sect. 3. We have really included the basically simple material of the present section mostly to illustrate that the concept of a dressed-atom laser existing in a symbiotic star cannot automatically be dismissed simply on the basis of a widespread belief that estimates of nonlinearly induced optical gain in these space objects would necessarily always yield values that fall far short of what would be required for such laser action to occur.

The reader is here reminded that in the astronomy/astrophysics literature one particular nonlinear optical scattering process *is* often postulated to occur near bright space objects. This is stimulated (or induced) Compton scattering (SCS). Although the unit scattering event in SCS is simply the well known effect of Compton scattering by an electron, it is widely assumed that the rate of occurrence of such events becomes enormously enhanced when the scattering ceases to

be purely linear and becomes stimulated. Thus, for example, Eq.(1) of Wilson (1982) expresses the probability p per unit time of scattering a photon from a state with wavevector $\mathbf{k}$ to another state with wavevector $\mathbf{k}_1$ as:

$$p = n(1+n_1)\left\{\frac{1}{2}r_e^2\left(1+\cos^2\phi\right)\delta\Big(\omega_1-\omega+\Delta\omega\Big)\right\} \times\left\{C^4\frac{d^3k_1}{\omega_1^2}\frac{d^3k}{(2\pi)^3}\right\}. \quad (12)$$

In this equation, the first two factors give the dependence of the scattering rate on the radiation intensities. The probability of destroying a photon in the initial state is proportional to n, the photon occupation number of that state, while the probability of creating a photon in the new state is proportional to $(1+n_1)$, with n_1 the occupation number in the new state. Compton scattering is a two-photon process, and the rate of power transfer in SCS from the primary beam to the secondary beam is proportional to the intensity product of the two beams. Hyper-Raman scattering is a three-photon process, and the rate of power transfer in SHRS from the two primary beams (*i.e.* the continuum beams) to the secondary beam is proportional to the intensity product of all three beams.

2.2. Could dressed-atom laser emission also occur on the C IV, N V, or O VI FUV doublet transitions in symbiotic stars?

For the pure hydrogen symbiotic star model of Sect. 2.1, it was shown that a sufficiently high rate of pumping for Lyα dressed-atom laser emission to occur could theoretically be achieved via SHRS conversion of incoherent Lyα light emerging from the Strömgren sphere. In order to examine whether dressed-atom laser emission could in principle also occur in symbiotic stars on the C IV, N V, or O VI FUV doublet transitions, one needs to have an approximate idea of how the nebular structure of the pure hydrogen symbiotic star model of Sect. 2.1 would be changed by allowing all other elements to be present in the red giant solar wind at densities corresponding to their cosmic abundance ratios. This would imply, for example, that the carbon atom (or ion, depending upon distance to the hot star) number density is everywhere $\approx 3.3 \times 10^{-4}$ times that for the H atoms (H^+ ions). A number of such ionization structure calculations were performed several years ago, when models for planetary nebulae were being developed (*e.g.* Fig. 2.6 of Osterbrock 1974; Figs. 3-5 of Hayes and Nussbaumer 1986). In a typical model for a planetary nebula, a centrally located blackbody radiation source with properties closely resembling those of a white dwarf in a symbiotic star system is assumed to be the ionizing source of a radiation bounded nebular shell of constant hydrogen density n(H) = n(H II) + n(H I). Such models have an inner radius r_i – *i.e.* a region of empty space is assumed to exist between the radiating source and the surrounding nebular shell. By contrast, in a symbiotic star the nebula which surrounds the hot star is contiguous with the latter. Despite this difference, we will here assume that results obtained for the ionization structures of planetary nebulae can also be utilized in the analysis of symbiotic stars.

We now focus specifically on the C IV doublet. In Fig. 3 of Hayes and Nussbaumer (1986), the ionization fractions for C are plotted as a function of distance from the inner radius r_i of a planetary nebula ionized by a hot star of temperature T = 200,000°K. From this figure one immediately sees that, even with a hot star temperature twice that assumed in the model of Sect. 2.1, *no* carbon ions more highly ionized than C V can be produced. The C V ion density is totally dominant within a spherical shell extending from r_i to roughly half the distance to the H I/H II interface. In the outer half of the ionized shell, the C IV ion density is dominant. The C IV/C V interface appears comparatively sharp. In incorporating the ionization fractions displayed in Fig. 3 of Hayes and Nussbaumer (1986) into the symbiotic star model of Sect. 2.1, we will assume the C IV/C V interface to occur in the latter at roughly one-tenth the hydrogen Strömgren sphere radius r_S, since a cooler radiation source implies a smaller C V region. At all radial distances less than that of the C IV/C V interface, C V ions would be constantly recombining with electrons, producing light at the C IV doublet transitions. However, the total C IV photon generation rate resulting from C V recombinations cannot exceed the rate at which the hot star emits C IV-ionizing photons, which for the parameters assumed in the model is roughly only two percent of the rate at which the same star emits H-atom-ionizing photons. Thus in Eq. (9), the value of the product $n_H I_p^2$ alone would be smaller in the case of C IV ions than the value estimated in Sect. 2.1 for H atoms by an amount that is at least equal to $(3.3 \times 10^{-4}) \times (0.02)^2 \times (100)^2 \approx 1.3 \times 10^{-3}$. This by itself would seem to rule out the possibility that dressed-atom laser emission could occur on the C IV, N V, or O VI FUV doublet transitions in symbiotic stars in a scheme that is exactly analogous to the one that was shown in Sect. 2.1 to be highly favorable for lasing on the H-atom Lyα transition.

Let us now consider the rate at which C IV ions would be excited to produce photons at the doublet transitions as a result of EIE. For simplicity, we now assume C IV to be the dominant carbon species throughout the entire hydrogen Strömgren sphere. Then the total rate ρ_{CIV}^{EIE} at which electrons located throughout the entire volume of the hydrogen Strömgren sphere produce photons at the C IV doublet transitions through collisions with C IV ions existing in the plasma is approximately given by the following expression:

$$\rho_{CIV}^{EIE} = \left(\frac{4\pi r_S^3}{3}\right) n_H v_e^{th} \sigma_e^{CIV} n_{CIV}, \quad (13)$$

where $n_{CIV} \approx (3.3 \times 10^{-4}) \times (1.2 \times 10^{10}) \approx 4 \times 10^6$ cm^{-3} is the C IV density everywhere within the Strömgren sphere, σ_e^{CIV} is the cross-section for electron impact excitation of C IV ions to the $2p\ ^2P_{1/2,3/2}$ states, and the other quantities are the same as in Eq. (7). We again approximate the value of σ_e^{CIV} by πa_o^2. The net result is that 5.3×10^{47} C IV photons are generated per second by EIE throughout the whole hydrogen Strömgren sphere. Thus the flux of C IV photons crossing r_S is about 6.3×10^{20} cm^{-2} sec^{-1}, representing an optical power of 809 W/cm^2. Interestingly enough, the optical power of this incoherent C IV line radiation is seen to be about six times greater than that of the incoherent Lyα radiation escaping the Strömgren sphere as

calculated in Sect. 2.1. This suggests that it is probably worth estimating if enough optical gain exists for C IV dressed-atom laser emission to occur in a path length $\sim r_S$ lying wholly within the Strömgren sphere. The pumping process would here again be SHRS, with the pump light itself being the C IV fluorescence generated by EIE, *i.e.* the quantity whose total rate of generation within the Strömgren sphere was calculated above in Eq. (13). As was the case in Sect. 2.1, it is here perhaps conceptually easiest first to assume that the laser light would originate near the hot star and would then become amplified while propagating outwards along the Strömgren sphere radii. Later, just as was eventually done in Sect. 2.1, one might attempt to refine the model by considering what would be the most favored laser beam propagation paths. Such an analysis will be given below. First, however, it is of interest to compare the 809 W/cm^2 figure for the C IV fluorescence intensity at the Strömgren sphere surface deduced above in *a priori* fashion with estimates of the same quantity that can be made via examination of spectra such as the one shown in Fig. 2.

When one views the spectrum of Fig. 2 at high amplifier gain, one sees that the average intensity of the background continuum emitted by the hot star between 1500 Å and 1600 Å that was recorded at the position of the detector is about 2 x 10^{-13} ergs cm^{-2} sec^{-1} Å^{-1}. One can roughly estimate what the actual continuum intensity should be at a distance r_S = 8.16 x 10^{12} cm from the hot star as follows. The hot star in Fig. 2 is the white dwarf in RR Tel, which has been recently estimated (see Nussbaumer and Dunn 1997) to have a temperature T = 140,000°K and a radius $R_h = 0.105\ R_\odot$. Therefore, at the hot star surface, and in the spectral vicinity of 1550 Å, the emitted continuum intensity should be about 4.55 x 10^{11} ergs cm^{-2} sec^{-1}Å^{-1}. At a distance r_S from the hot star, the corresponding intensity would be 3.65 x 10^5 ergs cm^{-2} sec^{-1} Å^{-1}. It thus follows that the intensities shown in Fig. 2 must be multiplied by roughly 1.82 x 10^{18} to get the values that would correspond to the intensities present at a distance r_S from the hot star. From Fig. 2 one would thus infer, for example, that at a distance r_S from the hot star, the intensity of the 1548-Å C IV doublet component would be about 11.4 W/cm^2, which is roughly 70 times less than the 809 W/cm^2 value calculated earlier as the C IV intensity crossing r_S that theoretically results from EIE alone. In principle, there could be many possible reasons for this discrepancy. For example, via the linear absorption and scattering processes responsible for interstellar reddening, roughly half the light emitted from RR Tel in the vicinity of 1550 Å would be undetectable from our solar system, since the value of E_{B-V} towards the former object is known to be about 0.08 (Jordan *et al.* 1994). Also, in the continuing discussion of C IV dressed-atom laser emission to be given below, a specific reason is suggested for the C IV emission intensity in a symbiotic star viewed at quadrature being notably less than when the system is viewed at superior conjunction. The orbiting plane of RR Tel is known to be close to the plane of the sky. Therefore, this object is always viewed at quadrature.

Let us now roughly estimate what would be the optical gain for a C IV dressed-atom laser beam propagating a distance r_S outwards from the hot star along a Strömgren sphere radius. We assume that the available SHRS pump power at radius r is $I_p(r) = 809\ (r/r_S)$ W/cm^2. Then, in propagating a distance r_S outwards from the hot star, the C IV laser beam intensity should be amplified by an amount e^{Σ}, where

$$\Sigma = (3.5x10^{-8})\frac{n_{CIV}\omega_{CIV}(809)^2}{n_H\omega_o(136)^2}\int_0^{r_S}(r/r_S)^2dr. \qquad (14)$$

Equation (14) follows from a comparison with the Lyα laser gain calculated in Sect. 2.1 via Eq. (9). The values of the parameters Δ, Γ, and μ are here taken to be the same as in the Lyα case. The net result is that $\Sigma = 8.7$, so that the C IV laser beam intensity would theoretically be amplified 6,090 times in propagating radially outwards from the hot star a length equal to r_S. Although the calculated laser gain in the case of C IV is not as high as that for Lyα (mainly because of the difference in densities), we assume that it is sufficient for dressed-atom C IV laser emission to occur in the symbiotic star here being modeled.

However, just as was done in Sect. 2.1, one should now consider what would be the most favored propagation directions for C IV lasing. It seems intuitively obvious that these again should coincide with the rays along which the red giant solar wind propagates. One would again expect there to be C IV laser beams propagating along these rays in two directions – towards and away from the red giant. The former would again converge to a spot on the red giant, being attenuated only via Rayleigh scattering by the H atoms in the solar wind (*vide infra*). The latter would propagate away from the symbiotic star system in a divergent pattern determined by the cone of solar wind rays in which the laser emission occurs. The dressed-atom laser beams propagating towards the red giant would be Doppler downshifted by the solar wind velocity. Those propagating in the other direction would be Doppler upshifted an equal amount. The cone defined by the C IV laser beams should be much narrower than in the Lyα case. This results from the fact that the C IV laser gain should be much higher for propagation directions that pass close to the hot star. For example, a C IV laser beam that just grazes the white dwarf would theoretically be amplified by an amount equal to (6,090) x (6,090) $\approx$ 37 x 10^6 in traversing from one side of the Strömgren sphere to the other, according to the calculation given above. On the other hand, a laser beam propagating in a direction that makes a tangent to the Strömgren sphere surface would experience zero optical gain. In the case of the Lyα laser beams discussed in Sect. 2.1, there would be very little difference in gain in these two directions.

Associated with the above scenario are some potentially serious conceptual difficulties, ones which we are unable to resolve satisfactorily at the present time. The two C IV dressed-atom laser beams (*i.e.* one for each of the $^2P_{3/2,1/2} \Leftrightarrow {}^2S_{1/2}$ doublet components) which propagate away from the red giant along a given solar wind ray are assumed to have roughly the same intensities within the Strömgren sphere as the two corresponding beams which propagate towards the red giant. Since the frequencies of the former beams are Doppler upshifted by the solar wind velocity, while those of the latter are Doppler downshifted an equal amount, what actually would here constitute the "dressed-atom" frequencies remains unclear, since the latter would depend upon which propagation direction one

is considering. In principle, one can try to circumvent this difficulty by conceptually dividing the total C IV ion population into two separate categories – one category comprising those ions that strongly interact resonantly with dressed-atom laser beams propagating in one direction, the other comprising ions that are resonant with beams propagating in the reverse direction. Such a seemingly artificial division of the C IV ion population into two separate categories is at least consistent with the tenuous nature of the solar wind cloud assumed in the model, which makes the collisional rate of C IV ions – even with protons and electrons - small compared to the rates of photonic processes. Another problem with the C IV dressed-atom-laser scenario of the present section is that it involves a V-type system, which in general allows dressed-atom fluorescence to occur (Sect. 3). In this connection, it should be noted that Narducci *et al.* (1990) have made *exact* calculations of the spontaneous emission and absorption properties of a driven V-type three-level system, and have shown that under certain conditions, depending upon the relative Rabi frequencies of the two driving laser beams, it is possible to reduce greatly *both* the linewidth and integrated intensity of the (five) fluorescent components surrounding each doublet transition. We are unaware how one should transfer results of these calculations to the complex situation represented by the C IV laser scenario. Relevant also to this problem of C IV dressed-atom fluorescence is the effect that was considered in the discussion of Hα dressed-atom laser emission in Sect. 2.1, namely, that such fluorescence should in principle be partly recyclable via SHRS re-pumping of the dressed-atom laser beams.

In the above scenario, the C IV dressed-atom laser radiation pattern forms a narrow cone whose axis is that of the symbiotic star and whose vertex is at the center of the red giant. According to this model, maximum C IV doublet radiation should be detected at superior conjunction in eclipsing symbiotic stars. At this phase, most of the doublet emission should appear blueshifted, unlike the case of the Hα emission shown in Fig. 10 where the strongest component is redshifted. For a symbiotic star with parameters roughly the same as those assumed for the model in Sect. 2.1, one would expect a relatively narrow cone of laser radiation to be produced. On the other hand, if the parameter X in Eq. (4) were larger, so that the ionized hydrogen nebular region were more like the one shown in the middle panel of Fig. 5, for example, the vertex angle of the C IV doublet emission radiation cone would be much larger. All this indicates that it would be of enormous benefit in evaluating this and other models to have available unsaturated, high signal-to-noise, spectral data showing exactly how the C IV emission doublet varies with phase in an eclipsing symbiotic star such as SY Muscae. In essence, it would be desirable to have access to C IV spectral data which would be the equivalent of the Hα data shown in Fig. 10.

It was mentioned earlier in the present section that, according to the C IV doublet emission model here being proposed, less intensity should be seen at quadrature than at superior conjunction. At quadrature, one is only able to detect fluorescence. If dressed-atom laser emission were completely absent in the model symbiotic star system, then the fluorescence seen at quadrature would correspond to the 809 W/cm^2 value calculated to be the intensity at r_S resulting from EIE. However, if dressed-atom laser emission were present, it is likely that in the volume of the Strömgren sphere that is occupied by the truncated cone of dressed-atom laser radiation, a large part of the EIE-produced fluorescence would be converted into dressed-atom laser radiation and would be transported out of the system. At quadrature, one would then mostly see EIE-generated fluorescence which is produced outside the volume through which the laser beams pass.

There is one particular striking spectrum that can be given a reasonable interpretation if a scenario analogous to the one presented above for C IV dressed-atom laser emission is assumed to hold when strong emission occurs in symbiotic stars on the 1032 Å, 1038 Å doublet of O VI ions. It is well known (see, for example, Schmid *et al.* 1999) that the presence of such O VI FUV doublet emission in symbiotic stars produces strong emission bands at $\approx$ 6825 Å and at $\approx$ 7085 Å via spontaneous Raman scattering by H atoms in the red giant solar wind. A recent visible spectrum of RR Tel that includes these emissions is shown in Fig. 11. By assuming a solar wind velocity of 60 km/sec, one calculates that in RR Tel there should be present a Raman emission band whose peak as seen from the vicinity of the Sun would occur at $\approx$ 6822 Å. This band would be produced by the interaction of the outgoing (*i.e.* upshifted) λ_{1032} O VI dressed-atom-laser beams with solar wind H atoms present in the vicinity of that portion of the Strömgren sphere surface that is most remote from the red giant. In calculating the above Raman wavelength, we used the generally accepted –62 km/sec value for the RR Tel-Sun relative velocity. For the value of ν_{1032}, we used 96,907.5 cm^{-1} (Moore 1971). With the same 60 km/sec solar wind velocity, one calculates that there should also be a Raman band whose wavelength seen from the Sun would be at $\approx$ 6825 Å. This would be produced by downshifted O VI dressed-atom laser beams propagating towards the red giant surface and interacting with solar wind H atoms present near the Strömgren sphere surface closest to the red giant. However, in some cases there would also be a third source of Raman emission. This would be the Raman scattering of the downshifted O VI dressed-atom laser beams that occurs as these beams converge upon a spot on the red giant surface - *i.e.* this would be Raman scattering by atoms present in the *photosphere* of the latter. The peak wavelength for this emission when viewed from the Sun would be $\approx$ 6832 Å. On the basis of these three calculated wavelengths, one can roughly account for the shape of the $\lambda''6825''$ band in Fig. 11. However, with the parameters that were chosen for the pure hydrogen symbiotic star model in Sect. 2.1, one should theoretically be unable to observe Raman emission arising from photospheric scattering in the red giant. This is because the Raman and Rayleigh cross-sections for excitation by light at 1032 Å are (Lee & Lee 1997) $\sigma_{Ram}(1032) = 7.5\sigma_T$, $\sigma_{Ray}(1032) = 34\sigma_T$, where $\sigma_T = 6.6 \times 10^{-25}$ cm^2 is the Thomson scattering cross-section. In the model of Sect. 2.1, the dressed-atom laser light would therefore be attenuated by roughly a million times in propagating from the Strömgren sphere surface nearest the red giant to the latter. On the other hand, if the hydrogen atom density in the solar wind were, for example, 10^7cm^{-3}, almost 99 percent of the laser beam intensity would reach the red giant. This would

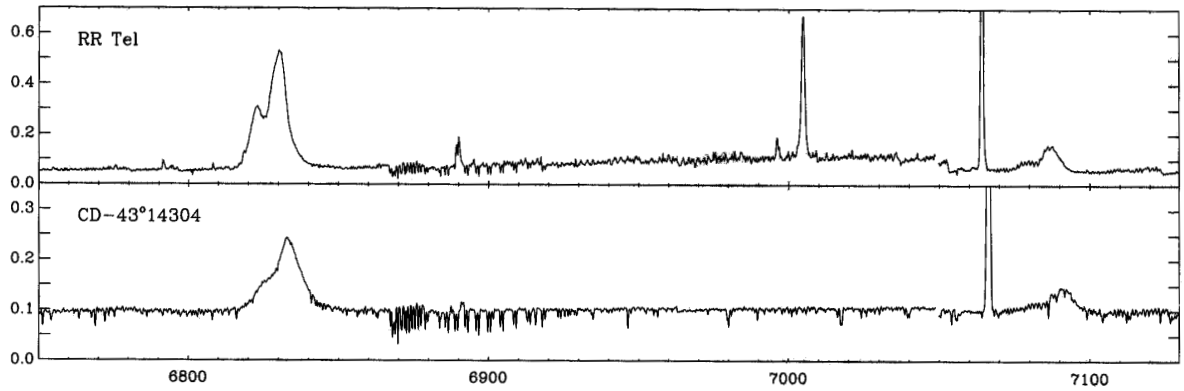

Fig. 11. RR Tel and CD-43°14304 high resolution spectra recorded near the broad Raman scattered O VI lines at ≈ 6825 Å and ≈ 7082 Å. The strong, narrow emission lines are due to [Ar V] λ7005 and He I λ7065. Reproduced from Fig. 9 of Schmid *et al.* (1999).

imply that the hydrogen density in RR Tel must be much less than that which was assumed in the model of Sect. 2.1.

Thus far in Sect. 2, it has been assumed that the nonlinear photonic process SHRS is the basic physical mechanism by which photons at the dressed-atom laser frequencies are generated in symbiotic stars, with the pump power being narrowband fluorescence produced via either I/R or EIE. For three main reasons, a coherently phased, dressed-atom gas is the ideal "acceptor" for photons "donated" via the SHRS process. (1) The dressed-atom gas allows all photons added to the laser beams via SHRS to propagate freely through space without attenuation (EIT). (2) The structure of the dressed-atom gas allows the SHRS pumping process to continue without reduced efficiency as the laser intensity level is increased, *i.e.* it prevents saturation of the pumping process from occurring. (3) Although SHRS can only efficiently convert incoherent pump light into coherent dressed-atom laser light when the frequencies of the former and the latter are very close together, the strong fluorescence that results from I/R or EIE is spectrally distributed in an optimal manner to allow this conversion to occur. All these effects only increase the likelihood that dressed-atom lasers are actually present in symbiotic stars. The three above statements also have interesting implications for the possible realization of a laboratory dressed-atom laser that would operate on almost exactly the same principles as those forming the basis for dressed-atom laser emission on FUV doublet transitions in symbiotic stars in the hypothesized scenario that has here been presented.

2.3. Stimulated radiation pressure scattering (SRPS): a nonlinear photonic process that could possibly be occurring in some symbiotic stars

In a *few* symbiotic stars, it has been observed that, around each component of the C IV (sometimes also N V) emission doublet, there occurs almost total absorption of the background continuum level in a comparatively narrow spectral region that is blueshifted from the associated resonance line by a small amount. A good example of a symbiotic star possessing such

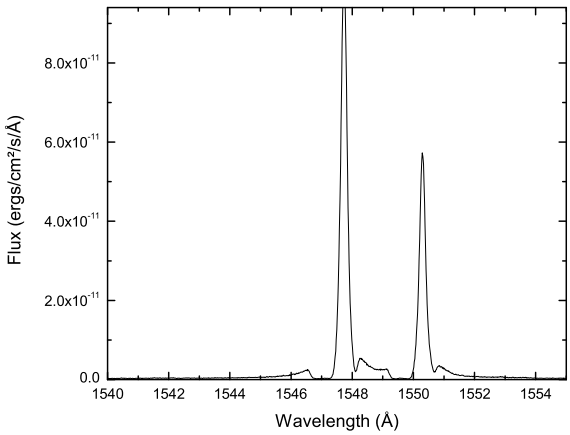

Fig. 12. *GHRS* spectrum of EG And. Data set: **Z27E0306T** downloaded from the *MAST Scrapbook* (http://archive.stsci.edu/scrapbook.html).

features is EG And (Fig. 12). At higher amplifier gain (Fig. 13), one sees that in this particular system there is also a pair of narrow redshifted absorption lines. In addition, the blueshifted absorption bands appear to possess a distinct two-component structure.

Vogel (1993) was the first to propose an interpretation for the absorption structure that could be seen around the C IV doublet in EG And spectra that were taken much earlier with *IUE*. He suggested that the blueshifted absorption bands represent what are known as P Cygni profiles, and he therefore concluded that the hot white dwarf in EG And loses material through its own fast, separate, solar wind. A similar conclusion was reached by Nussbaumer *et al.* (1995) for the symbiotic star AG Peg, again on the basis of blueshifted absorption bands appearing adjacent to FUV doublet emission lines. In the case of AG Peg, the blueshifted absorption structure occurred around the N V doublet.

P Cygni profiles of select ion resonances (*e.g.* C IV $\lambda\lambda$1548, 1551; Si IV $\lambda\lambda$1394, 1403; Al III $\lambda\lambda$1855, 1863) are often the dominant features in the FUV spectra of O-type (Walborn *et al.* 1985) and B-type (Walborn *et al.* 1985) stars. From Doppler-shift-based analyses of such profiles, astronomers have inferred that the corresponding ions are strongly accelerated radially away from the stars, reaching in some cases terminal velocities on the order of 1000 km/sec. As noted in Cassinelli (1979), current stellar wind theories fall into three broad classes: radiative models, coronal models, and hybrid models. In radiative models, transfer of photon momentum to the gas is assumed to occur through the opacity of the many strong FUV resonance lines that are present. Increased acceleration is believed to result from the progressive Doppler shifting of the line opacity into the unattenuated photospheric radiation field. The stellar wind in existing radiative models is thus assumed to be driven by a purely *linear* effect, commonly known as *radiation pressure*.

In a textbook description of an ideal P Cygni profile, the star's continuum light in a spectral region that is blueshifted with respect to the atom or ion resonance line is heavily absorbed. In a classic P Cygni profile, there also arises above the continuum level an emission peak which is roughly centered at the resonance line, but extends somewhat to both shorter and longer wavelengths from it. According to the standard model, the blueshifted absorption feature represents the effect of linear absorption by accelerated ions moving towards us in the line-of-sight. The broadened emission peak represents the net fluorescence the viewer would see arising from electronically excited, accelerated ions moving in all directions away from the star. In applying the standard P Cygni model to explain the profile seen in Fig. 13, one would naturally assume that the fluorescence of the accelerated C IV ions occurs as a result of EIE. This would imply, for example, that *some* of the background emission seen in the immediate vicinity of the two sharp redshifted absorption lines in Fig. 13 might represent EIE-induced fluorescence of *fully accelerated* C IV ions traveling directly away from us. In symbiotic stars, one should easily be able to see such fluorescence, because the white dwarf radius is so small. In O- and B-type stars possessing P Cygni profiles, such fluorescence would tend to be blocked from an observer's view by the star itself. For definiteness, we here now assume that some of the emission intensity occurring in the immediate vicinity of the two sharp redshifted absorptions in Fig. 13 represents EIE-induced fluorescence of fully accelerated C IV ions moving directly away from us. The ions emitting this fluorescence would all be located on the "other side" of the hot star from us. In principle, they could be as far away from the hot star as the Strömgren radius r_S. It then seems logical to assume that the *two redshifted absorption lines themselves must result from linear absorption of EIE-induced fluorescence originating in the hot star hemisphere farthest from us by fully accelerated C IV ions moving away from us in the same hemisphere.* On the basis of this hypothesis, one should be able to deduce directly from Fig. 13 the value of the terminal radial velocity attained by the accelerated C IV ions in EG And. The peak of the $^2P_{1/2} \Leftrightarrow {}^2S_{1/2}$ emission in Figs. 12 and 13 occurs at about 1550.3 Å. The associated redshifted absorption occurs at about

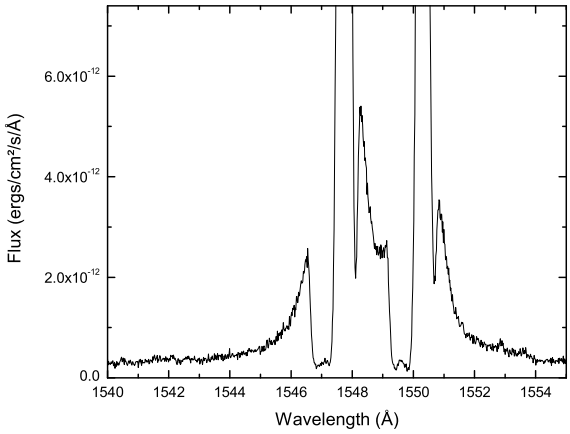

Fig. 13. Higher gain version of spectrum shown in Fig. 12.

1550.68 Å. Therefore, the terminal radial velocity of the C IV ions should be $\approx$ 73.5 km/sec.

Let us now consider the blueshifted absorptions appearing in Fig. 13. From this figure one sees that maximum absorption of the most blueshifted of the two distinctly separate components that together comprise the entire blueshifted region of absorption associated with the $^2P_{1/2} \Leftrightarrow {}^2S_{1/2}$ transition occurs approximately at 1549.5 Å. In the standard P Cygni model, this wavelength should correspond to Doppler shifted absorption by fully accelerated C IV ions moving towards us. However, the deduced terminal radial velocity of the C IV ions is here 154.9 km/sec, which is slightly more than twice the value deduced in the previous paragraph. Interestingly enough, if one were to assume that the other component which contributes to the blueshifted absorption region associated with the $^2P_{1/2} \Leftrightarrow {}^2S_{1/2}$ transition corresponds to the Doppler shifted absorption of fully accelerated C IV ions, then one would calculate a terminal velocity consistent with the value obtained earlier. The above mentioned other component maximally absorbs around 1549.9 Å, which would correspond to a terminal C IV velocity of $\approx$ 77 km/sec. Thus a serious inconsistency appears when one tries to interpret the blueshifted absorption components seen in Figs. 12 and 13 on the basis of a standard P Cygni model. In what follows, we shall attempt to resolve this discrepancy.

A model will now be proposed in which a *nonlinear* photomechanism both accelerates C IV ions present in the vicinity of the hot star and produces the most blueshifted of the two components that comprise each blueshifted region of strong absorption in Fig. 13. In this model, the redshifted component of each blueshifted region of absorption results from linear absorption by the accelerated ions, as do also the two sharp absorption lines appearing on the red wings of the doublet emission lines. The exact way in which the latter features are formed was discussed in detail earlier. In this model, the C IV ions that become accelerated must satisfy two requirements. (1) They must be positioned relatively close to the hot white dwarf. (2) They must have initial radial velocities with respect to the white

dwarf that are ≥ 0. C IV ions in the red giant solar wind that satisfy these two requirements all have the potential to become accelerated. *There is no need to assume a separate white dwarf solar wind in the model.* In the model, the C IV ion acceleration occurs in radial directions away from the white dwarf.

One important feature of the nonlinear photomechanism to be outlined below is that it would possess a definite pump power threshold. Only those ion species in a symbiotic star nebula for which this threshold is reached would be accelerated by the mechanism, and would therefore contain in their spectra the strong blueshifted absorption features seen in EG And. It was noted above that relatively few symbiotic stars possess these features. They are completely absent in RR Tel, for example.

The proposed new photomechanism is a stimulated scattering process, somewhat analogous to stimulated vibrational or rotational Raman scattering, yet different in that it involves *translational* motion of the scattering particles. Consider a photon (frequency ν_1, wavelength λ_1) from the hot star's continuum interacting with a C IV ion moving with a velocity whose radial component away from the white dwarf is v. Assume that there is also present a light wave (frequency ν_2, wavelength λ_2) propagating in the opposite direction, *i.e.* towards the hot star. If the intensity I_2 of the light wave at ν_2 is sufficiently great, there will exist a definite probability for the following nonlinear scattering event to occur. The photon at ν_1 will be absorbed, a photon at ν_2 will be added to the I_2 beam, and the radial velocity of the C IV ion will be increased to $v + \Delta v$, with all three events occurring *simultaneously.*

The equations for conservation of both momentum and energy are easily written down for the proposed scattering process. For the former, one has:

$$\frac{h}{\lambda_1} + \frac{h}{\lambda_2} = m_{ion}(\Delta v), \tag{15}$$

where m_{ion} is the mass of the C IV ion. The equation for conservation of energy is:

$$h\nu_1 \simeq h\nu_2 + m_{ion}v(\Delta v). \tag{16}$$

The functions $\nu_1(r)$, $\nu_2(r)$, and $v(r)$ must all vary with r, the distance from the white dwarf, in such a manner that Eqs. (15) and (16) are satisfied for all values of r, even when the above scattering process becomes *stimulated (vide infra).*

From Eq. (15), one has that:

$$\Delta v \simeq \frac{2h\nu}{cm_{ion}}. \tag{17}$$

Equation (17) states that the velocity increase Δv occurring in each scattering event is always the same, that is, Δv is not a function of r. It depends only on the properties of the ion being accelerated. For the C IV ion, one has that $\Delta v \simeq 43$ cm/sec. Although each nonlinear scattering event results only in a modest velocity increase for the ion being accelerated, the rate of occurrence of such events will be very large in those regions of the symbiotic star nebula near the hot star where the ions are being significantly accelerated, due to the scattering process becoming stimulated. This is now discussed.

One here envisions a wave at ν_2 starting at a distance from the hot star where the C IV ions have achieved their terminal radial velocities and propagating radially inwards towards the hot star, experiencing amplification via the nonlinear scattering process becoming stimulated. In order for the wave at ν_2 to experience optical gain, its frequency must remain roughly constant as it propagates inwardly towards the hot star. For the C IV system, there would actually be two I_2 beams, one for each doublet transition. It then seems most logical that the ν_2 values would be the actual C IV doublet frequencies. We will assume this to be the case.

The rate of stimulated scattering events occurring per unit volume at any distance r from the hot star will be equal to $\sigma(r)\phi_2(r)\phi_1(r)n_{ion}(r)$, where $\sigma(r)$ is the resonant nonlinear scattering cross-section (units $\mathrm{cm}^4\mathrm{sec}$) and where $\phi_1(r)$ is the continuum flux (photons cm^{-2} sec^{-1}) effective in pumping the stimulated scattering process at the distance r. If $\phi_1(r)$ were entirely due to blackbody continuum radiation emitted by the hot star, one would have $\phi_1(r) = K/r^2$, where K is a constant. The flux $\phi_2(r)$ in the beam(s) at ν_2 should grow rapidly with decreasing distance r according to the equation

$$-\frac{d\phi_2(r)}{dr} = \sigma(r)\phi_2(r)\phi_1(r)n_{ion}(r). \tag{18}$$

In this model, it is assumed that a steady state situation holds everywhere in the symbiotic star nebula. Thus, for example, the quantity $n_{ion}(r)$ is the density of C IV ions at distance r that have been accelerated to the velocity $v(r)$. Not included in $n_{ion}(r)$ are those C IV ions in the red giant solar wind that have not been accelerated by the nonlinear scattering process.

From Eqs. (15) and (16), one has

$$v \simeq \frac{h(\nu_1 - \nu_2)}{m_{ion}(\Delta\nu)} \simeq \frac{c(\nu_1 - \nu_2)}{2\nu}. \tag{19}$$

This equation appears to remove the confusion alluded to earlier related to the presence of two separate components in each blueshifted region of absorption in Fig. 13. The absorption band having the greater frequency offset from the resonance line is entirely due to the nonlinear process. However, Eq. (19) shows that the terminal velocity value deduced by applying standard Doppler analysis to this band must be divided by 2 in order to get the correct value.

Computer calculations should show exactly how the quantitities $v(r)$ and $\phi_2(r)$ depend upon r. In performing such a calculation, one would consider both Eq. (18) and the following equation, which represents the acceleration of the C IV ions via the stimulated scattering process:

$$v(r)\frac{dv(r)}{dr} = \sigma(r)\phi_1(r)\phi_2(r)\Delta v. \tag{20}$$

Additionally, there would have to be an equation of continuity relating the quantity $4\pi r^2 n_{ion}(r)v(r)$ to that fraction of the C IV red giant solar wind that becomes scattered via the nonlinear process here described. Only C IV ions moving in directions that pass close to the hot star could be so scattered. The easily determined terminal velocity would provide an additional boundary condition for the system of nonlinear equations governing the stimulated scattering process.

With the frequencies ν_2 being those of the doublet transitions, there would be plenty of light available via EIE for

"seeding" the I_2 beams at larger distances from the hot star. As already stated, as the I_2 beams continuously propagate inwardly towards the hot star, they become amplified via the nonlinear scattering process, which by now one sees could aptly be termed *stimulated radiation pressure scattering (SRPS)*. Maximum I_2 beam intensity would be attained at the hot star surface. Because of the small size of the hot star, most of this nonlinearly amplified light could pass around the latter and be in principle viewable from the "other side" of the hot star. One might therefore think that the I_2 light generated possibly accounts for a significant part of the doublet emission intensity one sees in the case of EG And, for example. However, a glance at Fig. 12 shows that the integrated continuum intensity removed by nonlinear absorption is evidently only a small fraction of the total integrated emission intensity observed. We can find no specific information regarding the orbital phase of EG And when the spectrum shown in Fig. 12 was recorded. (As was briefly noted in Sect. 2.1, EG And is an eclipsing symbiotic star.) However, by comparison with Fig. 3 of Vogel (1993), in which four *IUE* C IV doublet spectra recorded at different phases are shown, one surmises that in the case of Fig. 12, the phase of EG And must have been reasonably close to quadrature. If this is true, most of the doublet emission intensity one sees in this figure must be due to EIE, at least if one assumes that the C IV dressed-atom laser model outlined in Sect. 2.2 applies here. We conclude Sect. 2 by making the following prediction, which again hints at the value a complete series of high resolution spectra showing the variations that occur in the C IV profile in EG And with changes in orbital phase would have. One would predict that at superior conjunction the two narrow redshifted absorption lines seen prominently in Figs 12 and 13 would be absent. This is because it should not be possible for C IV ions to be accelerated in the direction of the red giant, because for these the "initial" radial velocities with respect to the hot star would be negative.

3. Fluorescence and absorption spectra of cascade-type dressed atoms

An energy level diagram similar to the one with which C-T&R introduce the concept of unperturbed, threefold-degenerate multiplicities $\varepsilon_{n,n'}$ is shown in Fig. 14. Wavy arrows pointing to the left or to the right describe the emission of a fluorescence photon on transitions *ab* or *bc*, respectively.

For cascade-type three-level atoms, Fig. 15 shows the unperturbed degenerate states of the multiplicity $\varepsilon_{n,n'}$ and indicates the couplings that are induced between these states by the presence of the two resonant light fields. The matrix element for the interaction Hamiltonian H_{int} that couples together two states of a multiplicity – for example, $|a, n+1, n'\rangle$ and $|b, n, n'\rangle$ - can generally be written as (see Cohen-Tannoudji *et al.* 1992, p. 415)

$$\langle b, n, n' | H_{int} | a, n+1, n' \rangle = -\frac{1}{2}\mu E(\omega_o) = \frac{1}{2}\hbar\omega_1, \qquad (21)$$

where μ is the *ab* transition dipole moment, $E(\omega_o)$ is the maximum value of the sinusoidally-varying electric field of the light beam at ω_o, and ω_1 is the Rabi frequency for this beam. (In the shorthand notation used in C-T&R, the quantity $\hbar$ appearing in Eq. (21) is taken to be equal to 1, as already mentioned.)

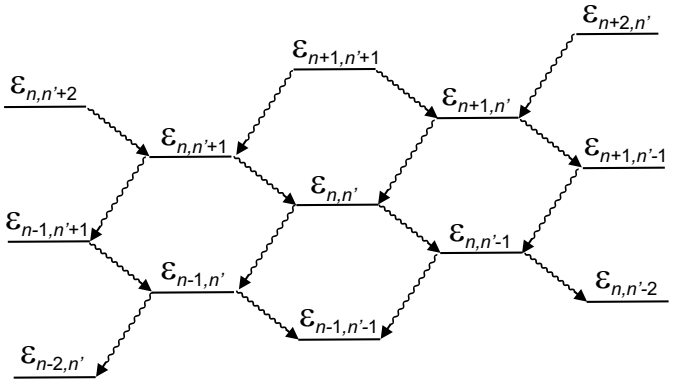

Fig. 14. Energy level diagram showing some of the (threefold degenerate) unperturbed multiplicities $\varepsilon_{n,n'}$. Wavy arrows pointing to the left or to the right depict the emission of a fluorescence photon on transitions *ab* or *bc*, respectively. After Fig. 3 of Cohen-Tannoudji & Reynaud (1977).

Diagonalization of the couplings inside each multiplicity $\varepsilon_{n,n'}$ is performed by C-T&R in the following manner. Two linear combinations of $|a, n+1, n'\rangle$ and $|c, n, n'-1\rangle$ are introduced which are respectively coupled and uncoupled to $|b, n, n'\rangle$. One first defines a "generalized Rabi frequency" Ω_1 in terms of the individual Rabi frequencies ω_1 and ω_1' of the two resonant laser beams.

$$\Omega_1 = \left(\omega_1^2 + \omega_1'^2\right)^{1/2} \qquad (22)$$

Defining an angle α by

$$\tan\alpha = \frac{\omega_1'}{\omega_1}, \qquad (23)$$

one then writes

$$\left|u, n, n'\right\rangle = \cos\alpha \left|a, n+1, n'\right\rangle + \sin\alpha \left|c, n, n'-1\right\rangle \qquad (24)$$

and

$$\left|v, n, n'\right\rangle = -\sin\alpha \left|a, n+1, n'\right\rangle + \cos\alpha \left|c, n, n'-1\right\rangle. \qquad (25)$$

Using Eq. (21), one readily verifies that $|v, n, n'\rangle$ is not coupled to $|b, n, n'\rangle$, while $|u, n, n'\rangle$ is coupled to this state with an amplitude $(1/2)\Omega_1$. C-T&R thus deduce that $\varepsilon_{n,n'}$ splits into three perturbed states $|i, n, n'\rangle\,(i = 1, 2, 3)$

$$\begin{aligned} \left|1, n, n'\right\rangle &= \frac{1}{\sqrt{2}}\left(\left|b, n, n'\right\rangle + \left|u, n, n'\right\rangle\right) \\ \left|2, n, n'\right\rangle &= \left|v, n, n'\right\rangle \\ \left|3, n, n'\right\rangle &= \frac{1}{\sqrt{2}}\left(-\left|b, n, n'\right\rangle + \left|u, n, n'\right\rangle\right) \end{aligned} \qquad (26)$$

with energies (measured with respect to the unperturbed energy of $\varepsilon_{n,n'}$) respectively equal to:

$$\begin{aligned} E_1 &= +\frac{1}{2}\Omega_1 \\ E_2 &= 0 \end{aligned} \qquad (27)$$

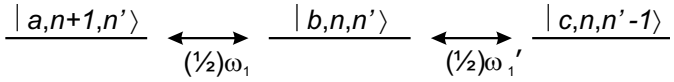

Fig. 15. Unperturbed degenerate states of the multiplicity $\varepsilon_{n,n'}$ for cascade-type three-level atoms. The double-headed arrows represent the couplings between the degenerate states, proportional to the Rabi frequencies ω_1 and ω_1'. After Fig. 4 of Cohen-Tannoudji & Reynaud (1977).

$$E_3 = -\frac{1}{2}\Omega_1.$$

These perturbed levels are shown in Fig. 16. Using Eqs. 24, 25, and 26, one can finally write the dressed-atom wavefunctions as linear combinations of the bare-atom wavefunctions for the cascade-type structure:

$$\begin{aligned}
\left|1, n, n'\right\rangle &= \frac{1}{\sqrt{2}}\left(\cos\alpha\left|a, n+1, n'\right\rangle + \left|b, n, n'\right\rangle\right) \\
&\quad + \frac{1}{\sqrt{2}}\left(\sin\alpha\left|c, n, n'-1\right\rangle\right) \\
\left|2, n, n'\right\rangle &= -\sin\alpha\left|a, n+1, n'\right\rangle + \cos\alpha\left|c, n, n'-1\right\rangle \qquad (28) \\
\left|3, n, n'\right\rangle &= \frac{1}{\sqrt{2}}\left(\cos\alpha\left|a, n+1, n'\right\rangle - \left|b, n, n'\right\rangle\right) \\
&\quad + \frac{1}{\sqrt{2}}\left(\sin\alpha\left|c, n, n'-1\right\rangle\right).
\end{aligned}$$

As a consequence of the assumption that the *ac* transition is forbidden, the only non-zero matrix elements of the atomic dipole moment operator M are $\mu = \langle a|M|b\rangle$ and $\mu' = \langle b|M|c\rangle$. Utilizing this fact, and making use of the wavefunction expansions appearing in Eqs. (28), one can easily evaluate the dipole matrix elements for all allowed spontaneous emission decays originating from each of the three perturbed levels $|i, n, n'\rangle$ of a given multiplicity $\varepsilon_{n,n'}$ and terminating on the various perturbed levels of lower-lying multiplicities. It becomes at once apparent that M couples $\varepsilon_{n,n'}$ only to adjacent multiplicities ($\varepsilon_{n\pm1,n'}$ or $\varepsilon_{n,n'\pm1}$). Equation (2.12) of C-T&R displays these dipole moments in the form of two simple tables. The individual dipole matrix elements are either zero, or are equal to μ or μ' multiplied by simple factors such as $(1/2)\cos\alpha$, $-(1/\sqrt{2})\sin\alpha$, etc. The individual spontaneous emission decay rates, obtained by squaring the various dipole matrix elements, are again either zero, or are equal to γ or γ' multiplied by simple factors such as $(1/4)\cos^2\alpha$, $(1/2)\sin^2\alpha$, etc. Here γ and γ' are the fluorescence decay rates of the two bare atom transitions $b \to a$ and $c \to b$.

For three-level cascade-type atoms, the allowed spontaneous emission decays from the three perturbed states of $\varepsilon_{n,n'}$ are shown as wavy arrows in Fig. 17. One instantly sees that the fluorescence spectrum $F_{ab}(\omega)$ observed on the transition $b \to a$ has five components at frequencies ω_o, $\omega_o \pm (1/2)\Omega_1$, and $\omega_o \pm \Omega_1$. A similar result holds for $F_{bc}(\omega)$, which exhibits five components at ω_o', $\omega_o' \pm (1/2)\Omega_1$, and $\omega_o' \pm \Omega_1$. The widths and the weights of the various fluorescence components are evaluated in C-T&R.

To obtain the strengths of either the dressed-atom fluorescence or the dressed-atom absorption components, one needs

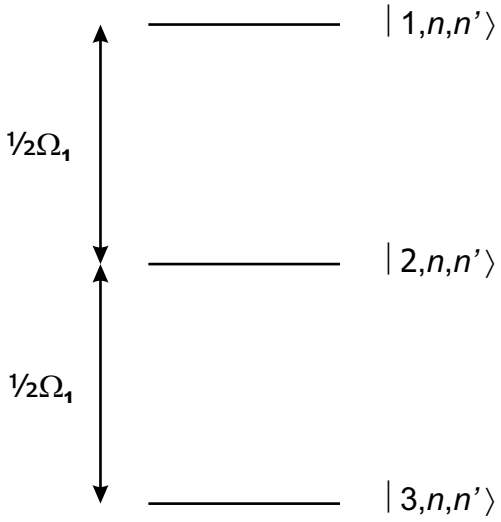

Fig. 16. Perturbed states of the multiplicity $\varepsilon_{n,n'}$, with a splitting determined by the generalized Rabi frequency $\Omega_1 = (\omega_1^2 + \omega_1'^2)^{1/2}$. After Fig. 5 of Cohen-Tannoudji & Reynaud (1977).

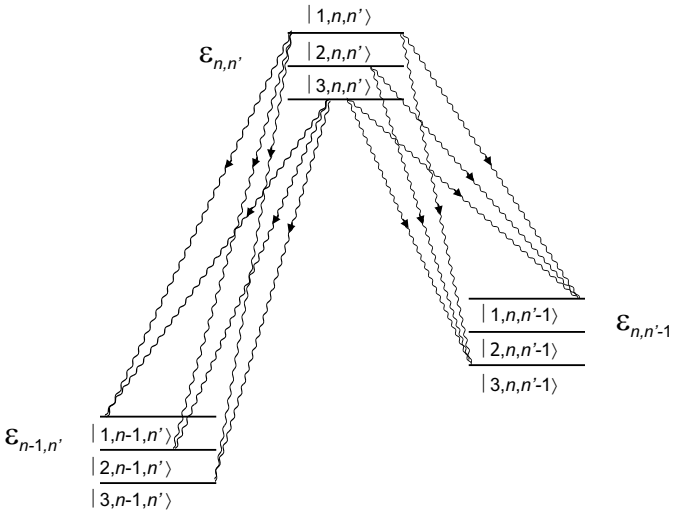

Fig. 17. Diagram showing all spontaneous emission decays (wavy arrows) which are allowed from the three perturbed states of $\varepsilon_{n,n'}$ to lower multiplicities in cascade-type dressed atoms. After Fig. 6 of Cohen-Tannoudji & Reynaud (1977).

to know the equilibrium populations π_i of the dressed-atom states (see Eq. (2)) Under the so-called "secular approximation" ($\Omega_1 \gg \gamma, \gamma'$), C-T&R show that the π_i can be obtained from simple rate equation considerations. The steady-state solution to these equations is found to be:

$$\pi_1 = \pi_3 = \frac{\gamma' \cos^2\alpha}{\gamma \sin^2\alpha + 2\gamma' \cos^2\alpha} \qquad (29)$$

$$\pi_2 = \frac{\gamma \sin^2\alpha}{\gamma \sin^2\alpha + 2\gamma' \cos^2\alpha}. \qquad (30)$$

With use of both Fig. 17 and Eqs. (29, 30), it is straightforward to predict the general appearance of absorption spectra of dressed cascade-type atoms.

For definiteness, let it be assumed that the ratio of Rabi frequencies of the resonant laser beams applied to the three-

level gas is such that $\omega_1 >> \omega_1'$. This would correspond to the assumption made in Sect. 2.1 that in symbiotic stars the Lyα dressed-atom laser beam intensities are much greater than those of the Hα dressed-atom laser beams. Then, to first order, one sees from Eqs. (23), (29), and (30) that $\pi_1 \approx \pi_3 \approx 1/2$, $\pi_2 \approx 0$. Through inspection of Fig. 17, one sees that no absorption should occur at either ω_o or ω_o', because of the essential equality of the populations in, for example, the states $|3, n-1, n'\rangle$ and $|3, n, n'\rangle$. This of course simply reflects the fact that a condition of EIT about each bare-atom transition automatically results from the presence of both applied resonant laser beams. From Fig. 17, it is apparent that EIT is equivalent to "saturation" occurring on transitions between dressed-atom states. For similar reasons, there is also no absorption at either $\omega_o \pm \Omega_1$ or $\omega_o' \pm \Omega_1$. Again from Fig. 17, one sees that the *only* linear absorption bands the cascade-type dressed-atom gas would display occur at $\omega_o' \pm (1/2)\Omega_1$. At $\omega_o \pm (1/2)\Omega_1$ only gain would be present, and not absorption. Any incoherent pumping light resonant with the latter transitions could only drive stimulated emission transitions that add photons to the incoherent pump source, while effectively *removing* them from the laser beam at ω_o. In the spectral vicinity of $\omega_o' \pm (1/2)\Omega_1$, however, power from the incoherent pumping source can in principle be transferred to the cascade system laser beams either via linear absorption, or else through a nonlinear absorption process such as SHRS. In Sect. 5, it will be shown that in symbiotic stars nonlinear pumping mechanisms are far more important than one based upon linear absorption. In Sect. 4, it will be seen that for Λ-type and V-type dressed-atom gases, only absorption occurs in the vicinities of both bare-atom transitions.

In all three types of dressed-atom systems, the *positions* of the absorption bands shift with increasing levels of laser power. However, the band *strengths* remain constant. This is the essential reason why saturation of the pumping efficiency of a three-level dressed-atom laser does not occur.

4. Spectral properties of Λ-type and V-type dressed-atom gases

In Narducci *et al.* (1990) the spontaneous emission and absorption properties of driven V-type three-level systems are calculated in considerable detail. General case formulas are derived that apply when the secular approximation ($\Omega_1 \gg \gamma, \gamma'$) is not valid, but a dressed-state description closely following the approach of C-T&R for the high intensity limit is also included. In a subsequent paper (Manka *et al.* 1991), corresponding spectral properties of the Λ and cascade models were investigated. The formulas for emission and absorption in the high-intensity limit contained in both of these papers generally agree with what can be discerned about driven three-level systems via inspection of dressed-atom energy level diagrams such as the one shown in Fig. 17. For example, formulas given in Manka *et al.* (1991) for the absorption spectra of the cascade model in the high intensity limit verify the conclusion drawn in Sect. 3 that absorption can be obtained in the vicinity of one transition, but not both.

For the Λ system, we are again interested in the high-intensity limit. Application of the two resonant laser fields again lifts the degeneracies of the multiplicities $\varepsilon_{n,n'}$, splitting them in exactly the same manner as shown in Fig. 16. Analogous to Eqs. (28) are equations expressing the dressed-atom wavefunctions as linear combinations of the bare-atom wavefunctions for the Λ system:

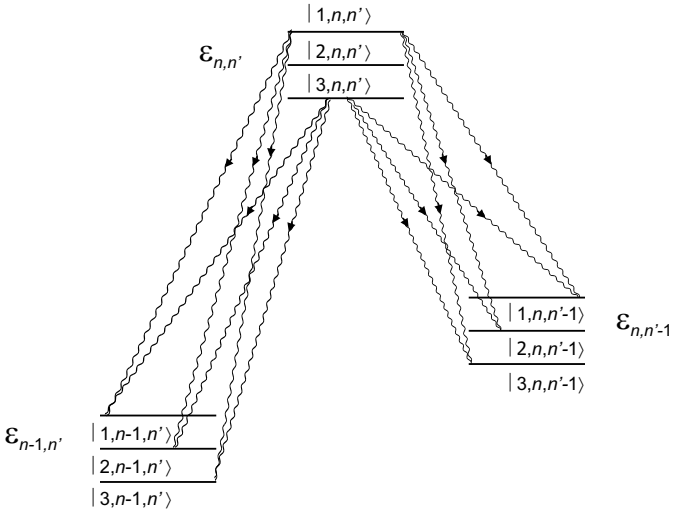

Fig. 18. Diagram showing all spontaneous emission decays which are allowed from the three perturbed states of $\varepsilon_{n,n'}$ to lower multiplicities in Λ-type dressed atoms.

$$
\begin{aligned}
|1,n,n'\rangle &= \frac{1}{\sqrt{2}}\left(\cos\alpha\,|a,n+1,n'\rangle + |b,n,n'\rangle\right) \\
&\quad + \frac{1}{\sqrt{2}}\left(\sin\alpha\,|c,n,n'+1\rangle\right) \\
|2,n,n'\rangle &= -\sin\alpha\,|a,n+1,n'\rangle + \cos\alpha\,|c,n,n'+1\rangle \qquad (31) \\
|3,n,n'\rangle &= \frac{1}{\sqrt{2}}\left(\cos\alpha\,|a,n+1,n'\rangle - |b,n,n'\rangle\right) \\
&\quad + \frac{1}{\sqrt{2}}\left(\sin\alpha\,|c,n,n'+1\rangle\right).
\end{aligned}
$$

Following the same procedure which led to the construction of Fig. 17, one can prepare an analogous diagram for the Λ system showing all the allowed spontaneous emission transitions that can occur from a given multiplicity $\varepsilon_{n,n'}$ (Fig. 18). It is apparent from Fig. 18 that, for the Λ system, the pattern of allowed spontaneous emissions around both bare-atom frequencies is the same as that around the *ab* transition for cascade-type dressed atoms. However, the equations for the Λ system that are analogous to Eqs. (29,30) for the cascade system are very much simpler. Simply by inspecting Fig. 18 one can see at once that, under the secular approximation, the following must hold: $\pi_1 = \pi_3 = 0$; $\pi_2 = 1$. The presence of applied laser beams at both ω_o and ω_o' has thus resulted in all the atoms in the gas becoming "coherently trapped" in the $|2, n, n'\rangle$ dressed-state levels. Moreover, this occurs for *all* values of $\tan\alpha$, the ratio of the individual laser Rabi frequencies (Eq. 23).

From inspection of Fig. 18, one can also instantly see why no fluorescence is emitted from a Λ-type dressed-atom gas. As is by now well known to scientists in the quantum electronics field, coherent trapping of Λ-type systems can be vividly

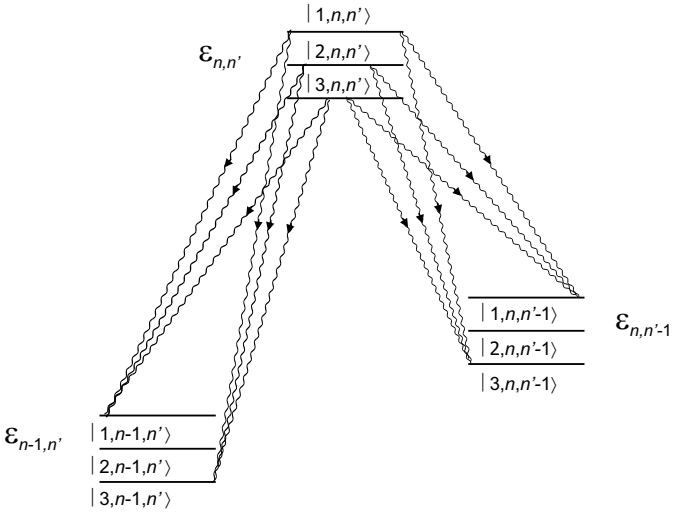

Fig. 19. Diagram showing all spontaneous emission decays which are allowed from the three perturbed states of $\varepsilon_{n,n'}$ to lower multiplicities in V-type dressed atoms.

demonstrated in the laboratory as a complete quenching of fluorescent emission from (bare-atom) level *b* when both laser beams are applied to a vapor cell, whereas when only one or the other of the beams is applied, bright fluorescence is seen. Among the earliest papers to discuss coherent trapping of Λ-type dressed atoms and to report laboratory demonstrations of this effect were Alzetta *et al.* (1976), Arimondo and Orriols (1976), and Gray *et al.* (1978).

Again, from mere inspection of Fig. 18, one can see that the linear absorption spectrum of Λ-type dressed atoms consists only of components at $\omega_o \pm (1/2)\Omega_1$ and $\omega_o' \pm (1/2)\Omega_1$. No linear gain is present around either of the bare-atom frequencies.

Figure 19 shows the analogous spontaneous emission diagram for V-type dressed atoms. Here the pattern of allowed spontaneous emission transitions about each bare atom frequency is seen to be the same as that about the *bc* transition in cascade atoms. The steady state solution for the dressed-atom level populations can be deduced from inspection of this figure to be $\pi_1 = \pi_3 = 1/2$, $\pi_2 = 0$, and this again holds for all intensity ratios of the two applied laser beams. The term "coherently trapped atoms" is therefore also a fitting description for V-type dressed atoms. The fluorescence spectrum in this case consists of a triplet around each of the bare-atom frequencies, with components at ω_o, $\omega_o \pm \Omega_1$, ω_o', and $\omega_o' \pm \Omega_1$. The linear spectrum of the dressed atoms here again contains only absorption bands occurring at $\omega_o \pm (1/2)\Omega_1$ and $\omega_o' \pm (1/2)\Omega_1$.

5. Stimulated Raman scattering (SRS) and stimulated hyper-Raman scattering (SHRS): realistic pumping mechanisms for dressed-atom lasers in symbiotic stars

One can utilize either Fig. 18 or 19 to evaluate the relative effectiveness of an optical pumping mechanism (either linear or nonlinear) that could in principle provide sufficient excitation for Λ- or V-type dressed-atom laser emission to occur. For the sake of definiteness, we here consider how amplification can be achieved in a tenuous gas of V-type or Λ-type dressed atoms irradiated by narrow-band fluorescence centered at ω_o and ω_o' resulting from I/R (and/or) EIE (*c. f.* Sects. 2.1 and 2.2). It will be assumed that the intensity of this fluorescence pump light is comparable to the calculated Lyα laser pumping light intensity in the model of Sect. 2.1. Also, as was done in the case of that model, it is here assumed that the pump light is spectrally distributed over a width $\Delta\nu_L \approx 6$ cm^{-1}.

There are three optical pumping mechanisms which potentially could provide a basis for amplification of both applied laser beams in a dressed-atom laser: linear pumping by the incoherent fluorescent light, stimulated broadband Raman scattering (SRS), and stimulated hyper-Raman scattering (SHRS). Consider first the effect of linear pumping of V-type dressed-atom gases via absorption of IR- (and/or) EIE-produced fluorescence in the absorption bands at $\omega_o \pm (1/2)\Omega_1$. An individual photonic event occurring in this type of process might be, for example, absorption of a continuum photon at $\omega_o - (1/2)\Omega_1$ accompanied by excitation of a dressed atom from state $|1, n-1, n'\rangle$ to state $|2, n, n'\rangle$. While through this event the number of ω_o photons dressing the atom is temporarily increased by 1, the energy thus gained by the dressed-atom system soon becomes irretrievably lost via the four fluorescent transitions indicated in Fig. 19. The *rate* at which dressed atoms are excited from $|1, n-1, n'\rangle$ to $|2, n, n'\rangle$ via linear absorption is given approximately by the fluorescence pumping flux within the dressed-atom absorption bandwidth times the maximum cross-section of the dressed-atom absorption band. Taking the latter to be $(\lambda^2/2\pi)(\Delta\nu_n/\Delta\nu_D)$, its value at Ly$\alpha$ would be $\approx$ 1.2 x 10^{-14} cm^2, if the Doppler width $\Delta\nu_D$ of the dressed atoms is here for simplicity also assumed to be 6 cm^{-1}. In the pure hydrogen symbiotic star model of Sect. 2.1, the flux of Lyα fluorescent photons crossing the surface of the Strömgren sphere was calculated to be 8.3 x 10^{19} photons cm^{-2} sec^{-1} ($\equiv$136 W/cm^2)**.** Hence, the rate at which a dressed atom in state $|1, n-1, n'\rangle$ is linearly excited to state $|2, n, n'\rangle$ would be no greater than $\approx 10^6$ sec^{-1}, which is approximately three orders of magnitude less than the net rate of fluorescent decay from $|2, n, n'\rangle$. Thus, one must evidently look beyond linear absorption to find an effective symbiotic star dressed-atom-laser pumping mechanism.

Consider next stimulated Raman scattering (SRS) as a possible pumping mechanism for dressed-atom space lasers. SRS is a stimulated two-photon process that efficiently converts pump light into coherent light called the Stokes wave. It works equally well whether or not the pump light is coherent (*vide infra*). In SRS, the unit step involves simultaneous absorption of a pump photon and creation of a Stokes-wave photon, with an atom moving from a populated initial level to an unpopulated terminal level, and with total energy being exactly conserved in the step. From the V-type dressed-atom energy level diagram (Fig. 19), one sees that four separate SRS photonic processes which generate Stokes waves at the bare-atom frequencies are theoretically possible. One such process would involve the simultaneous absorption of a continuum photon at $\omega_o - (1/2)\Omega_1$ accompanied by emission of a photon at ω_o. From Fig. 19, one sees that such SRS events would originate from populated dressed-atom $|1, n, n'\rangle$ levels and terminate on un-

populated dressed-atom $|2, n, n'\rangle$ levels. Light at ω_o would also be generated via the SRS process in which continuum light at $\omega_o + (1/2)\Omega_1$ is absorbed. Here the events would originate from populated $|3, n, n'\rangle$ levels and terminate again on unpopulated $|2, n, n'\rangle$ levels. Two similar SRS transitions occurring about ω'_o could, in principle, provide amplification at that frequency. All four SRS processes must originate from the upper levels shown in Fig. 19 in order to terminate on unpopulated levels. There are also four potential SRS processes starting from the upper levels that terminate on unpopulated levels but have Stokes-wave frequencies different from the bare-atom frequencies. These would, however, be discriminated against, because the SRS transition probability is proportional to the instantaneous power in the Stokes wave, and the latter can only build up if the Stokes-wave frequency stays constant.

In the above discussion, both the SRS pump radiation and the Stokes-wave emission were considered to be spectrally coincident with specific dressed-atom resonant transitions. However, for the purposes of highlighting and explaining some subtle, but nonetheless important, physical properties of the SRS process, it will be helpful for us to assume temporarily that the following additional constraints apply: (1) The fluorescence pump light bandwidth $\Delta\nu_L$ is significantly larger than the dressed-atom Doppler width $\Delta\nu_D$. (2) The incoherent fluorescence pump light is applied in the same direction that the generated Stokes waves propagate. One then has optimum conditions for the occurrence of *broadband* SRS, an effect known in the quantum electronics field for more than thirty years.

In broadband SRS it is observed that in the backward direction (*i.e.* counter-propagating pump and Stokes waves) the gain coefficient is proportional to $(\Delta\nu_L + \Delta\nu_D)^{-1}$, while in the forward direction, *in the absence of dispersion of the Stokes wave relative to the pump wave*, the gain is proportional to $(\Delta\nu_D)^{-1}$ alone. For such relative dispersion effects to be negligible, the pump spectrum should be significantly detuned from the transition between the initial state **1** and the intermediate state **2**, as depicted in Fig. 20, for example. When this is so, the threshold for SRS is completely independent of pump bandwidth, and just depends upon the total pump power. For a pump spectrum that doesn't overlap the intermediate state resonance (Fig. 20), the SRS threshold varies as the square of the frequency offset. When the pump spectrum overlaps the intermediate state resonance, the SRS threshold depends upon the *spectral density* of the pump, and one sees a threshold dependence as shown in Fig. 21.

Scientists in the quantum electronics field frequently explain the pump-bandwidth-independent SRS threshold behavior observed in the off-resonant case, and also the fact that SRS can evidently be excited just as easily by incoherent light as by coherent light, by postulating that, whenever SRS does occur, the Stokes-wave radiation is generated with a time-varying phase that exactly equals the time-varying phase of the pump radiation, no matter how randomly-varying the latter may be (*c.f.* the equations shown in Fig. 20). This is the so-called "phase locking" postulate. However, according to Raymer *et al.* (1979), its theoretical basis is not particularly well understood. When the equations shown in Fig. 20 are substituted into the nonlinear equations describing the growth of the Stokes wave in SRS, the phases of the pump and Stokes-wave fields exactly cancel, and do not therefore enter at all into the determination of the SRS Stokes-wave gain, and hence threshold value. However, a pump field E_L in Fig. 20 having a constant amplitude ε_L but a stochastically-varying phase φ_L which abruptly changes at a rate $\dot{\varphi}_L = 2(\Delta\nu_L)$ would have a spectral bandwidth $\Delta\nu_L$, and should therefore be viewed as a "broadband" source. This is the so-called "phase diffusion" model of stochastic light. It is frequently employed in nonlinear optics calculations (*e.g.* in Raymer *et al.* (1979), and in references

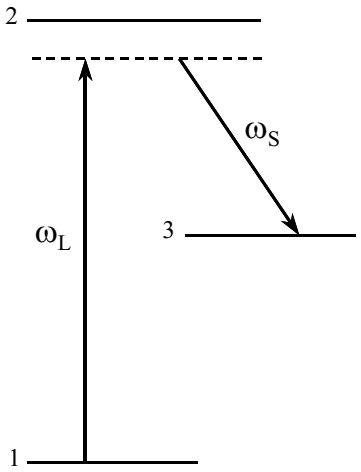

Fig. 20. Diagram of a broadband SRS process in which the pump beam spectrum is offset from the intermediate state resonance. The phase $\phi_L(z, t)$ of the pump beam electric field is here assumed to be stochastically varying.

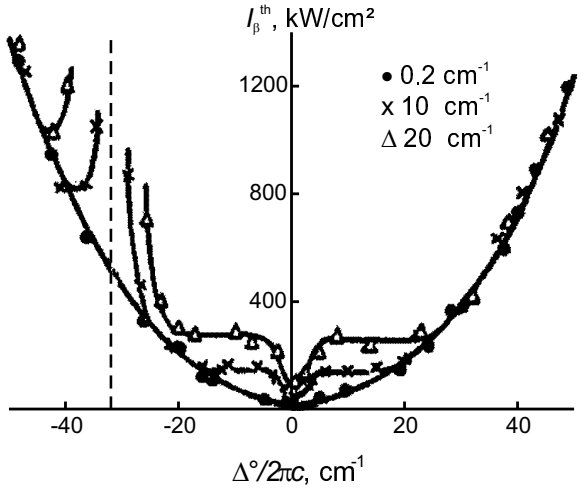

Fig. 21. Experimental measurements by Korolev *et al.* (1978) showing the dependency of SRS threshold on both the center frequency and bandwidth of the pump beam spectrum, when the latter overlaps the intermediate state resonance. The pump beam bandwidths utilized are indicated. After Fig. 2 of Korolev *et al.* (1978).

cited in that work), because the mathematics involved is relatively tractable.

Under the assumption that phase locking occurs in SRS, it can be easily shown that a certain nonlinear photonic loss process – one that *a priori* would seem to have the potential to cancel entirely the laser gain produced by SRS – can actually be neglected. This is *two-photon absorption* (TPA). In the V-type dressed-atom diagram (Fig. 19), the TPA process could be represented, for example, by a simultaneous two-photon absorption step originating from $|3, n-1, n'\rangle$, proceeding upwards via $|3, n, n'\rangle$,and terminating on $|2, n+1, n'\rangle$. However, whereas the randomly-varying pump and Stokes-wave phase shifts cancel in SRS, they add in TPA. This continually keeps the sum of the pump and Stokes-wave photon energies detuned from the two-photon resonance, thus lowering the TPA transition probability.

Basically, all the properties of SRS outlined above are consistent with it occurring in a gas of V-type dressed atoms excited in an end-pumped configuration by photons from a sufficiently intense, resonant, incoherent light source. However, an interesting observation that results from a comparison of Figs. 18 and 19 suggests that while SRS should be possible with Λ-type systems, it should not occur with V-type systems. A general requirement for an effective dressed-atom-laser pumping mechanism is that it must be able to "donate" photons to the two separate laser beams at ω_o and ω_o' in such a manner as to keep the atoms in the gas coherently phased (*i.e.* "dressed"). Having all atoms in the gas coherently phased implies that the phases of the two resonant laser beams traversing the system and phasing the atoms must be the same, or at least must differ by only a fixed amount. This would imply that if broadband SRS is the mechanism that donates the photons at ω_o and ω_o' to the system, the difference in phases of the two generated Stokes waves, no matter how rapidly the individual phases may vary, must be constant in time. Now consider Fig. 18. It is apparent that *each* SRS pumping transition (*e.g.* the transition from $|2, n-1, n'\rangle$ to $|3, n, n'\rangle$) is two-photon coupled to Stokes-wave transitions at *both* frequencies ω_o and ω_o' (*e.g.* the transitions from $|3, n, n'\rangle$ to $|3, n-1, n'\rangle$ and $|3, n, n'-1\rangle$). This implies that when SRS occurs, the two Stokes waves generated are excited by a common source of pump light. Under the assumption that phase locking occurs, both Stokes waves would therefore have the same phase. On the basis of Fig.19, however, one clearly cannot make the same argument. One is therefore led to conclude, for example, that broadband SRS could not be the effective pumping mechanism for C IV, N V, or O VI dressed-atom lasers that possibly could exist in symbiotic stars.

On the basis of the preceding discussion, broadband SRS would still seem to be a viable photonic scheme for pumping the symbiotic star dressed-atom Lyα laser of Sect. 2.1, a Λ-type system which was analyzed on the assumption that the laser gain results entirely from SHRS. One now should therefore compare calculated optical gains for the two processes SRS and SHRS. A general formula for the SRS gain coefficient can again be found in Hanna *et al.* (1979) and is:

$$G_R = g_R I_L = \frac{2\pi^2 r_e^2 c^2}{\hbar} \frac{n_H \omega_S}{(\Delta\omega_D)} \frac{f_{32} f_{12}}{\Omega_{23}\Omega_{21}} \frac{I_L}{(\Omega_{21}-\omega_L)^2} \quad , \quad (32)$$

where r_e is the classical electron radius $r_e \simeq 2.82$ x 10^{-15} m, the f's and Ω's are oscillator strengths and angular frequencies of the transitions shown in Fig. 20, and I_L is the Lyα fluorescence power that end-pumps the hydrogen gas. We assume here that the pump light and Stokes-waves are collinear, so as to satisfy the conditions required for broadband SRS to occur. For I_L and n_H, we choose the same values used in Sect. 2.1, *i.e.* 1.36 x 10^6 W/m^2 and 1.64 x 10^{16} m^{-3}, respectively. We again assume the spectral width of the pump light to be 6 cm^{-1}, but we here take the hydrogen atom Doppler width $\Delta\nu_D$ to be 3 cm^{-1} ($\Delta\omega_D$ =5.65 x 10^{11} radians/sec), so as to satisfy the $\Delta\nu_L > \Delta\nu_D$ requirement of broadband SRS. The f numbers in Eq. (32) are here both assumed to be 1.

As explained earlier, Eq. (32) strictly speaking only applies when the pump is significantly detuned from the transition to the intermediate state, as depicted in Fig. 20, for instance. However, here we are assuming that the pump spectrum is centered on the pumping transition. Fortunately, from Fig. 21 it can be inferred that one should be able to determine approximately the SRS gain coefficient in the present case from Eq. (32) by substituting a value ≈ 6 cm^{-1} for the quantity $(\nu_{21} - \nu_L)$. The net result, when all the above numerical substitutions are made, is that $G_R \approx 2.7$ x 10^{-7} m^{-1}. *This is a gain coefficient roughly 7.7 times greater than the (already large) value for G_{HR} which was calculated in Sect. 2.1!*

Because it involves a simpler nonlinear process, it is likely that the SRS gain calculation given here should be more accurate than the one given in Sect. 2.1 for Lyα laser gain due to SHRS. At this stage, it appears that one should probably simply conclude that both SRS-pumped and SHRS-pumped Lyα dressed-atom lasers could exist in symbiotic stars. One would expect the SRS-pumped lasers, which favor end-pumping configurations, to propagate mostly in directions that are orthogonal to the H I/H II interface. The spectrum of an SRS-pumped dressed-atom laser beam should be virtually identical with that of the fluorescence which pumps it - *i.e.* no pronounced spectral narrowing should occur. One therefore is again impelled to ask what would be the astrophysical consequences (aside from facilitating Hα dressed-atom-laser beam generation, as discussed in Sect. 2.1) of having Lyα dressed-atom laser emission occur in symbiotic stars. One answer is that such laser beams would provide a rapid and effective means for *radiation transport* in symbiotic stars, *i.e.* the removal of energy from the immediate proximity of the ionized region that surrounds the hot member of such systems. Looking beyond symbiotic stars, it is apparent that there is here a viable nonlinear mechanism having the potential to generate intense Lyα laser light that could propagate directly away from other bright space objects, such as OB stars or perhaps even quasars.

We now present a somewhat analogous dressed-atom analysis that would apply to the case of SHRS. Here V-type atoms are considered, since SHRS is apparently the only effective pumping mechanism for these systems. Figure 22 is a schematic diagram showing the basic SHRS processes which are assumed to occur around *both* bare-atom frequencies ω_o and ω_o' in a dressed-atom space laser, although only processes around the former frequency are shown. The two photonic processes shown at the left would generate photons at ω_o. The two

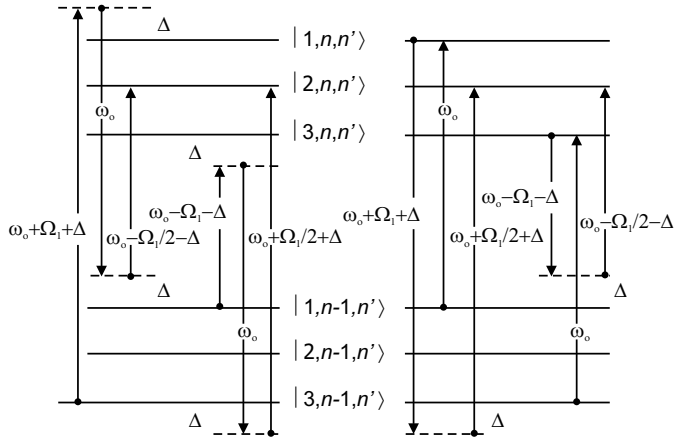

Fig. 22. Schematic diagram showing the basic SHRS processes which are assumed to occur around both bare-atom frequencies ω_o and ω_o' in a dressed-atom space laser. (Only processes around the former frequency are shown.) The two processes shown at the right are competing ones (see text).

processes shown at the right are competing ones, which would act to remove photons at ω_o from the generated Stokes wave. As stated above, and as can be seen from Fig. 19, there are equivalent processes that occur around ω_o'. As can also be seen from Fig. 19, there are various "cross processes" that can occur. An example of the latter would be the following. Starting with an atom in $|3, n-1, n'\rangle$, a continuum photon at $\omega_o - \Omega_1 - \Delta$ is absorbed, a photon at ω_o' is emitted, and a continuum photon at $\omega_o' - \Omega_1/2 - \Delta$ is absorbed, with all events occurring simultaneously and with the atom ending up in the unpopulated level $|2, n, n'\rangle$. In Fig. 22, the value of Δ is arbitrary, in principle extending out to a significant fraction of the pump fluorescence bandwidth $\Delta\nu_L$.

The following argument is based upon the assumption that, when a stimulated hyper-Raman scattering process occurs, the phases of the three participating waves are related in a manner analogous to the condition $\phi_L(z,t) - \phi_S(z,t) = 0$ linking the phases of the pump and the generated Stokes-wave light in broadband SRS (Fig. 20). Considering the waves participating in the SHRS processes shown in Fig. 22, and also those (not shown in Fig. 22) which involve frequencies around ω_o', one would write:

$$\phi_c(\omega_o + \Omega_1 + \Delta) - \phi(\omega_o) + \phi_c(\omega_o - \Omega_1/2 - \Delta) = 0, \quad (33a)$$

$$\phi_c(\omega_o - \Omega_1 - \Delta) - \phi(\omega_o) + \phi_c(\omega_o + \Omega_1/2 + \Delta) = 0, \quad (33b)$$

$$\phi_c(\omega_o + \Omega_1 + \Delta) - \phi(\omega_o') + \phi_c(\omega_o' - \Omega_1/2 - \Delta) = 0, \quad (33c)$$

$$\phi_c(\omega_o - \Omega_1 - \Delta) - \phi(\omega_o') + \phi_c(\omega_o' + \Omega_1/2 + \Delta) = 0, \quad (33d)$$

$$\phi_c(\omega_o' + \Omega_1 + \Delta) - \phi(\omega_o') + \phi_c(\omega_o' - \Omega_1/2 - \Delta) = 0, \quad (33e)$$

$$\phi_c(\omega_o' - \Omega_1 - \Delta) - \phi(\omega_o') + \phi_c(\omega_o' + \Omega_1/2 + \Delta) = 0, \quad (33f)$$

$$\phi_c(\omega_o' + \Omega_1 + \Delta) - \phi(\omega_o) + \phi_c(\omega_o - \Omega_1/2 - \Delta) = 0, \quad (33g)$$

$$\phi_c(\omega_o' - \Omega_1 - \Delta) - \phi(\omega_o) + \phi_c(\omega_o + \Omega_1/2 + \Delta) = 0, \quad (33h)$$

with $\phi_c(\omega)$ being the phase of a small bandwidth of continuum light at ω used in pumping the various SHRS processes.

From Eqs. (33c) and (33e), it follows that $\phi_c(\omega_o + \Omega_1 + \Delta) = \phi_c(\omega_o' + \Omega_1 + \Delta)$. From Eqs. (33d) and (33f), it likewise follows that $\phi_c(\omega_o - \Omega_1 - \Delta) = \phi_c(\omega_o' - \Omega_1 - \Delta)$. Since Δ is of arbitrary value, it then follows from (for example) Eqs. (33a) and (33c) that $\phi(\omega_o) = \phi(\omega_o')$. *This last equation represents a necessary and sufficient condition for the atoms to remain "dressed" as the light intensity at both narrow-band frequencies ω_o and ω_o' continues to increase due to SHRS.*

By contrast, for the first of the two competing processes shown at the right in Fig. 22 to be correctly phased for optimum transition probability, one would require $\phi(\omega_o) - \phi_c(\omega_o + \Omega_1 + \Delta) + \phi_c(\omega_o + \Omega_1/2 + \Delta) = 0$. From Eq. (33a), this would then require that $\phi_c(\omega_o - \Omega_1/2 - \Delta) = -\phi_c(\omega_o + \Omega_1/2 + \Delta)$. Since this last equation does not follow from Eqs. (33a-33h), one is able to conclude that rapid phase fluctuations of the waves involved in the competing process keep it continually detuned from exact three-photon resonance, thus greatly decreasing its transition probability. The reader will recognize that this argument is essentially the same as the one used earlier to show that TPA could be neglected in the case of broadband SRS.

6. Summary

A "dressed-atom" gas, *i.e.* a gas of three-level atoms coherently phased by the application of collinearly propagating resonant laser beams tuned to the "bare-atom" frequencies ω_o and ω_o', is shown to be an ideal medium for greatly amplifying both applied laser beams, provided there exists a suitable independent pumping mechanism which can "donate" photons to the two laser beams both at a sufficiently high rate and in a manner that allows the atoms in the gas to remain "dressed". If the optical gain per unit propagation length is high enough, such a system will generate intense beams of coherent light (*i.e.* laser light) via amplification of either weak, resonant, "seed" light or optical noise. A dressed-atom gas possesses two striking and important properties that make it an ideal laser medium. (1) It displays a remarkable transparency (EIT) at both ω_o and ω_o' that allows the amplified beams to propagate in space without being attenuated. (2) It has a characteristic quantum level structure that allows the pumping process to continue to occur without loss of efficiency as the power in the beams being amplified increases, *i.e.* it prevents saturation of the pumping process from occurring.

Two nonlinear photonic processes are identified as suitable dressed-atom-laser pumping mechanisms: stimulated hyper-Raman scattering (SHRS) and stimulated broadband Raman scattering (SRS). Both processes are shown to be effective means of converting incoherent pump light into coherent dressed-atom laser light, provided that the frequencies of the former and the latter are close together. This requirement is optimally satisfied, for example, if the incoherent pump light is the strong fluorescence at ω_o and ω_o' produced via electron impact excitation (EIE) in an ionized plasma, since pump and laser frequencies would here differ at most by the Doppler width $\Delta\nu_D$. It is assumed throughout the present paper that the source of pump light is narrow-band fluorescence generated either via EIE or through ionization/recombination (I/R). Through inspection of dressed-atom energy level diagrams, it

is deduced that SRS could occur in the case of Λ-type systems, but not in V-type systems, whereas SHRS could in principle occur in both types of system. This conclusion is based on the specific abilities of the two above pumping processes to keep the atoms of a coherently phased gas "dressed" as photons are "donated" to the two laser beams. There is an additional constraint for SRS pumping in Λ-type systems - the pump radiation must be applied collinearly with the propagation direction of the dressed-atom laser beams, *i.e*. an end-pumping configuration must be employed. No such restriction holds for SHRS pumping; the pump radiation can in this case be applied in an isotropic manner along the whole amplification path length of the laser beams.

In this paper, it is investigated whether such dressed-atom laser systems could possibly be present in symbiotic stars. The latter are compact space objects having both an extremely intense, point like, source of pumping energy (the white dwarf member) as well as (by astronomical standards) very high densities of atomic hydrogen gas (as much as 10^{10} cm^{-3}) present in the red giant solar wind in the vicinity of the hot star – both features that *a priori* would make such systems favorable astronomical environments for the occurrence of dressed-atom laser emission. The calculated optical gains for Lyα dressed-atom laser beams pumped via SRS are found to be extremely large, making it appear quite likely that such lasers could indeed be present in symbiotic stars. SRS-pumped Lyα dressed-atom laser beams in symbiotic stars would be expected to have the following properties. The laser beam spectrum should be virtually identical with that of the pumping radiation, with the latter being the Lyα fluorescence generated via I/R and EIE in the ionized hydrogen region that surrounds the white dwarf. The SRS-pumped Lyα laser beams should originate at, and propagate away from, the H I/H II interface in directions that are roughly normal to the latter. At any distance r from the white dwarf, the intensities of the Lyα laser beams should be comparable to that which one would expect for Lyα fluorescence in the complete absence of dressed-atom laser emission, both quantities falling off as $1/r^2$. Transmission of Lyα fluorescence energy away from the H I/H II interface would normally involve photonic propagation along circuitous random-walk paths necessitated by the combined effects of elastic scattering by H atoms in the red giant solar wind and diffusion. However, if the fluorescence were entirely converted close to the H I/H II interface into Lyα dressed-atom radiation, the energy would then be transported at the speed of light in straight-line paths leading directly away from the interface. In essence, such a conversion process would constitute an effective channel for *radiative transport* in symbiotic stars. It is entirely possible that this evidently robust mechanism is also operative in the case of other very bright space objects, such as OB stars or perhaps even quasars.

The optical gain for SHRS-pumped Lyα dressed-atom laser emission in symbiotic stars is also calculated to be very large, although not as large as the gain for SRS-pumped laser emission. The presence of either one in a symbiotic star theoretically should facilitate the occurrence of cascade-type Hα dressed-atom laser emission, although calculations of optical gain are here much more difficult to perform than in the case of Lyα laser emission alone. Balmer-α radiation is strongly seen in symbiotic stars, and in those systems which are known to be eclipsing, the Hα spectral profiles display puzzling variations with changes in orbital phase. A speculative Hα-laser-based interpretation is offered for such spectral data recorded in the case of SY Mus.

The possibility that dressed-atom laser emission can at least partially account for the intense FUV doublet emissions of C IV, N V, or O VI ions that are frequently seen in symbiotic stars is examined. These isoelectronic ions all have the same V-type level structure, so that the only available dressed-atom-laser pumping mechanism for them would be SHRS. Rough estimates are made of the likelihood that C IV dressed-atom laser emission occurs in symbiotic stars. The calculated optical gain is much less than for SHRS-pumped Lyα lasers, and seems marginal at best. Amplification should here occur in straight-line paths contained within that part of the ionized hydrogen plasma in which C IV is the dominant carbon species. The pump light would be C IV fluorescence generated via EIE in the C IV-dominant region. In our model, a surprisingly large amount of such C IV fluorescence is generated, the calculated optical power crossing the H I/H II interface being roughly six times the value estimated for Lyα fluorescence. The lower calculated C IV-laser gain simply reflects the relative abundance (3.3×10^{-4}) of carbon to hydrogen in the red giant solar wind. As a result of the marginal gain, one would expect C IV dressed-atom laser emission to occur in a relatively narrow beam, defined by a cone of solar wind propagation rays whose axis is that of the symbiotic star, and whose surface passes reasonably close to the white dwarf. Laser emission would occur within the C IV-dominant region along the solar wind rays in both directions. Laser beams propagating away from the red giant would be Doppler blueshifted by the solar wind velocity and should be seen in eclipsing symbiotic stars at superior conjunction. Laser beams propagating towards the red giant would converge to a spot on the photosphere of the latter, and should be hidden from direct view at all orbital phases. These beams would be Doppler redshifted by the red giant solar wind velocity. At quadrature, all observable doublet emission should represent fluorescence. A possible manifestation of bi-directional laser beams occurring in symbiotic stars might be the split profiles one sees in the red Raman bands in symbiotic stars having strong O VI doublet emission. In the case of RR Tel, the Raman profile can be roughly explained with the assumption of a 60 km/sec solar wind velocity.

A new nonlinear process, stimulated radiation pressure scattering (SRPS), is proposed to explain the observation that, in a few symbiotic stars, there occurs almost total absorption of the background continuum level in two comparatively narrow spectral regions, each blueshifted by the same amount from a component of an FUV doublet. A high quality C IV spectrum of EG And is analyzed on the basis of this new photonic scheme. Contributing viability to the proposed process is the fact that it simply explains why the above mentioned blueshifted absorption bands possess a distinct two-component structure. The same nonlinear model also accounts for the presence in EG And of a pair of narrow redshifted absorption lines. In addition, it is somewhat reassuring that the predicted two-

component structure of the blueshifted absorption bands directly follows from equations that represent conservation of both momentum and energy in the unit scattering process.

Acknowledgements. We are much indebted to the two reviewers who carefully pointed out to us that the original manuscript we had submitted on this subject contained major errors of omission and some questionable physics. One reviewer noted that we had totally ignored the process of EIE in symbiotic stars, and suggested that we revise our manuscript to include estimates of the importance of this process. The result is that EIE now emerges in our model as the major pumping source for the proposed dressed-atom lasers. The second reviewer noted that no estimates of optical gain in symbiotic stars were contained in our original submission. That omission has now been remedied with results we find to be interesting and illuminating.

PPS is grateful to IBM Research management for allowing him the use of office facilities as an IBM Fellow Emeritus.

References

Alzetta G., Gozzini A., Moi, L. *et al.* 1976, Nuovo Cimento, 36B, 5
Arimondo E., & Orriols G. 1976, Nuovo Cimento Lett., 17, 333
Cassinelli J.P. 1979, ARA&A, 17, 275
Cohen-Tannoudji C., & Reynaud S. 1977, J. Phys. B, 10, 2311
Cohen-Tannoudji C., Dupont-Roc J., & Grynberg G. 1992, Atom-Photon Interactions (Wiley-Interscience, New York, Chichester, Weinheim, Brisbane, Singapore, and Toronto)
Eikema K.S.E., Walz J., & Hänsch T.W. 2001, Phys. Rev. Lett., 86, 5679
Fulton D.J., Shepherd S., Moseley R.R. *et al.* 1995, Phys. Rev. A, 52, 2302
Gray H.R., Whitley R.M., & Stroud C.R. 1978, Opt. Lett., 3, 218
Hanna D.C., Yuratich M.A., & Cotter D. 1979, Nonlinear Optics of Free Atoms and Molecules (Springer-Verlag, Berlin, Heidelberg, and New York)
Hayes M.A., & Nussbaumer H. 1986, A&A, 161, 287
Jordan S., Mürset U., & Werner K. 1994, A&A, 283, 475
Korolev F.A., Mikhailov V.A., & Odintsov V.I. 1978, Opt. Spectroscopy, 44. 535
Lee K.W., & Lee H.-W. 1997, MNRAS, 292, 573
Manka A.S., Doss H.M., Narducci L.M. *et al.* 1991, Phys. Rev. A, 43, 3748
Moore C.E. 1971, Atomic Energy Levels, Vol. 1, Nat. Stand. Ref. Data. Ser., Nat. Bur. Stand. (U.S.), 35
Munari U. 1993, A&A, 273, 425
Narducci L.M., Scully M.O., Oppo G.-L., *et al.* 1990, Phys. Rev. A, 42, 1630
Nussbaumer H., & and Dunn T. 1997, A&A, 323, 387
Nussbaumer H., Schmutz W., & Vogel M. 1995, A&A, 293, L13
Osterbrock D.E. 1974, Astrophysics of Gaseous Nebulae (Freeman, San Francisco)
Raymer M.G., Mostowski J., & Carlsten J.L. 1979, Phys. Rev. A, 19, 2304
Schmid H.M., Krautter J., Appenzellar I., *et al.* 1999, A&A, 348, 950
Schmutz W., Schild H., Mürset U., *et al.* 1994, A&A, 288, 819
Seaquist E.R., Taylor A.R., & Button S. 1984, ApJ, 284, 202
Sorokin P.P., & Glownia J.H. 2002, A&A, 384, 350
Taylor A.R., & Seaquist E.R. 1984, ApJ, 286, 263
Vogel M. 1993, A&A, 274, L21
Walborn N.R., Nichols-Bohlin J., & Panek R.J. 1985, International Ultraviolet Explorer Atlas of O-Type Spectra from 1200 to 1900 Å (NASA Reference Publication 1155)
Walborn N.R., Parker J.W., & Nichols J.S. 1995, International Ultraviolet Explorer Atlas of B-Type Spectra from 1200 to 1900 Å (NASA Reference Publication 1363)
Wilson D.B. 1982, MNRAS, 200, 881